

# JGR Atmospheres

## RESEARCH ARTICLE

10.1029/2019JD032004

### Key Points:

- $1.9 \pm 0.3$  MtC of fossil fuel CO<sub>2</sub> was emitted in Baltimore-Washington during February 2015 based on data collected during seven aircraft flights
- Four bottom-up inventories indicate  $2.2 \pm 0.3$  MtC of fossil fuel CO<sub>2</sub> was emitted, in good agreement with our top-down estimate
- The uncertainty from a single flight segment was  $\pm 38\%$  ( $1\sigma$ ); data from seven flights yielded a precision of 16% at the 95% confidence level

### Supporting Information:

- Supporting Information S1

### Correspondence to:

D. Y. Ahn,  
aahndo@umd.edu

### Citation:

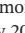











Ahn, D. Y., Hansford, J. R., Howe, S. T., Ren, X. R., Salawitch, R. J., Zeng, N., et al. (2020). Fluxes of atmospheric greenhouse-gases in Maryland (FLAGG-MD): Emissions of carbon dioxide in the Baltimore, MD-Washington, D.C. area. *Journal of Geophysical Research: Atmospheres*, 125, e2019JD032004. <https://doi.org/10.1029/2019JD032004>

Received 6 NOV 2019

Accepted 11 APR 2020

Accepted article online 15 APR 2020

## Fluxes of Atmospheric Greenhouse-Gases in Maryland (FLAGG-MD): Emissions of Carbon Dioxide in the Baltimore, MD-Washington, D.C. Area

D. Y. Ahn<sup>1</sup> , J. R. Hansford<sup>2</sup>, S. T. Howe<sup>3,4</sup> , X. R. Ren<sup>3,5,6</sup> , R. J. Salawitch<sup>1,3,5</sup> , N. Zeng<sup>3,5</sup> , M. D. Cohen<sup>6</sup> , B. Stunder<sup>6</sup>, O. E. Salmon<sup>7,8</sup> , P. B. Shepson<sup>7,9</sup> , K. R. Gurney<sup>10</sup> , T. Oda<sup>11,12</sup> , I. Lopez-Coto<sup>13</sup> , J. Whetstone<sup>14</sup>, and R. R. Dickerson<sup>3</sup> 

<sup>1</sup>Department of Chemistry and Biochemistry, University of Maryland, College Park, MD, USA, <sup>2</sup>Department of Computer Science, University of Maryland, College Park, MD, USA, <sup>3</sup>Department of Atmospheric and Oceanic Science, University of Maryland, College Park, MD, USA, <sup>4</sup>Now at Areté, Arlington, VA, USA, <sup>5</sup>Earth System Science Interdisciplinary Center, University of Maryland, College Park, MD, USA, <sup>6</sup>National Oceanic and Atmospheric Administration Air Resource Laboratory, College Park, MD, USA, <sup>7</sup>Department of Chemistry, Purdue University, West Lafayette, IN, USA, <sup>8</sup>Now at Lake Michigan Air Directors Consortium, Madison, WI, USA, <sup>9</sup>School of Marine and Atmospheric Sciences, Stony Brook University, Stony Brook, NY, USA, <sup>10</sup>School of Informatics, Computing, and Cyber Systems, Northern Arizona University, Flagstaff, AZ, USA, <sup>11</sup>Global Modeling and Assimilation Office, NASA Goddard Space Flight Center, Greenbelt, MD, USA, <sup>12</sup>Goddard Earth Sciences Research and Technology, Universities Space Research Association, Columbia, MD, USA, <sup>13</sup>Engineering Laboratory, National Institute of Standards and Technology, Gaithersburg, MD, USA, <sup>14</sup>Special Programs Office, National Institute of Standards and Technology, Gaithersburg, MD, USA

**Abstract** To study emissions of CO<sub>2</sub> in the Baltimore, MD-Washington, D.C. (Balt-Wash) area, an aircraft campaign was conducted in February 2015, as part of the Fluxes of Atmospheric Greenhouse-Gases in Maryland (FLAGG-MD) project. During the campaign, elevated mole fractions of CO<sub>2</sub> were observed downwind of the urban center and local power plants. Upwind flight data and Hybrid Single Particle Lagrangian Integrated Trajectory (HYSPLIT) model analyses help account for the impact of emissions outside the Balt-Wash area. The accuracy, precision, and sensitivity of CO<sub>2</sub> emissions estimates based on the mass balance approach were assessed for both power plants and cities. Our estimates of CO<sub>2</sub> emissions from two local power plants agree well with their Continuous Emissions Monitoring Systems (CEMS) records. For the 16 power plant plumes captured by the aircraft, the mean percentage difference of CO<sub>2</sub> emissions was  $-0.3\%$ . For the Balt-Wash area as a whole, the  $1\sigma$  CO<sub>2</sub> emission rate uncertainty for any individual aircraft-based mass balance approach experiment was  $\pm 38\%$ . Treating the mass balance experiments, which were repeated seven times within 9 days, as individual quantifications of the Balt-Wash CO<sub>2</sub> emissions, the estimation uncertainty was  $\pm 16\%$  (standard error of the mean at 95% CL). Our aircraft-based estimate was compared to various bottom-up fossil fuel CO<sub>2</sub> (FFCO<sub>2</sub>) emission inventories. Based on the FLAGG-MD aircraft observations, we estimate  $1.9 \pm 0.3$  MtC of FFCO<sub>2</sub> from the Balt-Wash area during the month of February 2015. The mean estimate of FFCO<sub>2</sub> from the four bottom-up models was  $2.2 \pm 0.3$  MtC.

## 1. Introduction

A major increase in the atmospheric abundance of CO<sub>2</sub> since the industrial revolution—with significant positive perturbation to the radiative forcing of climate—has resulted in a rise of global mean surface temperature over the past century (Stocker et al., 2013). A large number of studies that clarified the detrimental impact of global warming and resulting climate change on Earth's ecosystem have spurred individual nations to mitigate greenhouse gas (GHG) emissions under the Paris Climate Agreement (Salawitch et al., 2017). Along with the efforts by most of the world's nations, the role of cities in GHG mitigation has become even more important given the recent U.S. federal decision to pull back from the Paris Climate Agreement (United Nations, 2017). Currently, the state of Maryland is on track for reducing consumption-basis GHG emissions by 25% in 2020 and 40% in 2030 relative to emissions in 2006 (Maryland Department of the Environment [MDE], 2015). Washington, D.C. has set a plan to reduce consumption-basis GHG emissions by 50% in 2032 and by 100% in 2050 relative to 2006 emissions (Department of Energy & Environment, 2018).

With increasing GHG mitigation efforts, scientific research to improve the quantification and attribution of carbon sources in urban areas has become more important (Duren & Miller, 2012; Hutyra et al., 2014; Patarasuk et al., 2016). According to UN-Habitat (2011), more than 70% of global CO<sub>2</sub> emissions related to energy usage comes from urban areas. Also, measuring CO<sub>2</sub> in urban areas is more tractable than measuring CO<sub>2</sub> in countries, because the CO<sub>2</sub> signal from cities is intense and localized (Gratani & Varone, 2005; Idso et al., 2001). Various measurement techniques, data analyses, and modeling methods have been collectively used to study CO<sub>2</sub> emission in urban areas. Among many U.S. cities, the Indianapolis area was chosen as one of the first testbed sites to develop and evaluate a framework to study urban GHG emissions, given its relatively simple topography and isolation from other large cities (Davis et al., 2017; Whetstone, 2018). The Indianapolis Flux Experiment (INFLUX, <https://www.nist.gov/topics/greenhouse-gas-measurements/indianapolis-flux-experiment>) has successfully developed and improved the mass-balance method and the inversion framework, called “Top-down” approaches, as well as inventory data-based emission models such as Hestia, a “Bottom-up” approach (Gurney et al., 2017; Lauvaux et al., 2016; Turnbull et al., 2015; Turnbull et al., 2018; Whetstone, 2018). Along with INFLUX, several projects with similar aims have been conducted in other cities. The Megacities Carbon Project was designed to quantify carbon emissions in some of the world’s largest cities, including Los Angeles, Paris, and San Paulo (Bréon et al., 2015; Feng et al., 2016; Newman et al., 2016). Urban GHG emissions from the Boston area (Sargent et al., 2018) and Salt Lake City (McKain et al., 2012; Strong et al., 2011) have also been extensively investigated.

The Fluxes of Atmospheric Greenhouse-Gases in Maryland (FLAGG-MD) project is part of the National Institute for Standards and Technology (NIST) U.S. Northeast Corridor testbed which, in its first phase, is focused on the Baltimore, Maryland (MD)-Washington, D.C. (Balt-Wash) area (Lopez-Coto et al., 2017; Mueller et al., 2018; <https://www.nist.gov/topics/northeast-corridor-urban-test-bed>). Taking a lead from the successful deployment of INFLUX, the FLAGG-MD project aims to understand and quantify emissions of CO<sub>2</sub>, CH<sub>4</sub>, and CO in the Balt-Wash area. While FLAGG-MD is similar in many ways to INFLUX, the geography of the Balt-Wash area engenders the following complications. The Balt-Wash area is part of the U.S. Northeast Corridor, which includes other major cities such as Boston, New York City, and Philadelphia. Also, the Balt-Wash area is located southeast of the Appalachian Mountains and northwest of the Chesapeake Bay, such that mesoscale circulations complicate the atmospheric transport of urban GHG emissions. Several large power plants upwind of the Balt-Wash area can episodically increase the spatiotemporal variability of the background mole fractions of CO<sub>2</sub>. The Balt-Wash urban testbed consists mainly of aircraft campaigns conducted in collaboration with Purdue University (Lopez-Coto et al., 2020; Ren et al., 2018; Salmon et al., 2017; Salmon et al., 2018), along with several other assets: installations of low cost CO<sub>2</sub> sensors (Martin et al., 2017), meteorological data assimilation, modeling of tower-based observations (Martin et al., 2019; Mueller et al., 2018), and incorporation of data from the Orbiting Carbon Observatory 2 (OCO-2).

In this study, emissions of CO<sub>2</sub> from the Balt-Wash area are quantified using the FLAGG-MD aircraft campaign data set obtained during the month of February 2015. Section 2 describes the aircraft campaign, the mass balance approach, and various models used in this study. In section 3.1, source apportionment of the plumes of CO<sub>2</sub> observed by the aircraft is presented. In section 3.2, the impact of plume transport from out-of-state power plants on the aircraft observations is investigated. In section 3.3, the accuracy and precision of the aircraft-based mass balance estimates are evaluated using the Continuous Emissions Monitoring Systems (CEMS) records of two local power plants. Section 3.4 discusses the uncertainty from mass balance parameters. In section 3.5, differences in the CO<sub>2</sub> emission rate among our mass balance estimate, other previously published bottom-up/downscaling model estimates, and the state of Maryland emission inventory are investigated.

## 2. Methods

### 2.1. Instrumentation

The University of Maryland (UMD) Cessna 402B aircraft was equipped with a cavity ring-down spectroscopic (CRDS) analyzer (Picarro Model G2401-m) that is used to measure the dry air mole fraction of CO<sub>2</sub>. Measurements of CO<sub>2</sub> were calibrated on the ground as well as during the flight using an onboard calibration system with two cylinders of standard gases certified by National Institute of Standards and Technology

(NIST). These cylinders contained CO<sub>2</sub> of 369.19 and 445.78 μmol mol<sup>-1</sup> (parts per million or ppm). A diaphragm pump was installed to pull the ambient air from the nose of the Cessna through a rear-facing Perfluoroalkoxy alkanes Teflon tube (O.D = 0.95 cm and I.D = 0.64 cm), at a total flow rate of 10 L min<sup>-1</sup>. The CRDS analyzer was connected to the main sample line via a Tee connection, allowing air to be pumped continuously through the analyzer at a rate of 400 ml min<sup>-1</sup>. We tested the stability of the analyzer by sampling a tank of breathing air continuously while the aircraft climbed from 50 to 3,500 m altitude—the standard deviations of CO<sub>2</sub> were very small, near the measurement precision limit of the Picarro instrument. The UMD aircraft was also equipped with instruments to measure SO<sub>2</sub>, NO<sub>2</sub>, NO, O<sub>3</sub>, aerosols, and meteorological variables. A more detailed description on the instrumentation can be found in Ren et al. (2018). The Purdue Duchess aircraft was equipped with a CRDS analyzer (Picarro Model G2301-m) for measurements of CO<sub>2</sub> and a Best Air Turbulence (BAT) probe for measurements of the three-dimensional wind field. A more detailed description of the instrumentation on the Purdue Duchess aircraft can be found in Salmon et al. (2018).

To examine the sensitivity of our mass-balance emission estimation of CO<sub>2</sub> emissions (described in section 2.5) to the measurement uncertainties, 1σ uncertainties of the temperature, pressure, and CO<sub>2</sub> mole fraction measurements were propagated into the mass balance equation. The 1σ absolute uncertainty of temperature measurements from both UMD and Purdue flight instruments was determined to be 2.0 K, based upon a comparison of temperature measurements made from the two aircraft during a wingtip-to-wingtip flight segment conducted on 19 February 2015. For the 1σ uncertainty of the pressure measurements for the UMD flights, the reported instrument uncertainty of 0.25 hPa was used. For the Purdue flights, 1σ uncertainty was determined to be 1.6 hPa based upon a comparison of measured pressure versus calculated barometric pressure. For the 1σ uncertainty of the CO<sub>2</sub> measurements, the reported instrument uncertainty of 0.1 ppm was used for data collected by both the UMD and Purdue instruments.

## 2.2. Aircraft Research Flight Design

For this study, the Balt-Wash area is defined as a rectangularly shaped region enclosed by the four coordinates of 38.23°N 76.67°W, 39.46°N 75.86°W, 39.87°N 77.04°W, 38.63°N 77.86°W (154 × 111 km<sup>2</sup>, see Figure 1). The defined study area consists of large populated regions, within and surrounding the cities of Baltimore, MD and Washington, D.C. The total population within the study area was 8,153,000 in year 2015 based on Gridded Population of the World (GPWv4) data (CIESIN, 2018). Seven major power plants (all within either the states of Maryland or Virginia) and a dense road network including major highways such as the Capital Beltway ring (I-495), the Baltimore Beltway (I-695), and interstate highway I-95 all lie within the study area. According to the Maryland GHG inventory, total of 18.8 MtC (million tons carbon) of fossil fuel CO<sub>2</sub> (FFCO<sub>2</sub>) was emitted from Maryland during year 2014 (MDE, 2016).

The UMD aircraft conducted a total of nine research flights (UMD RF1–9) in February 2015. Figure 1 shows all of these flight tracks, and supporting information Figure S1 shows individual flight tracks. During seven research flights (UMD RF1–6 and RF8) northwesterly winds prevailed, while a northeasterly wind was present on UMD RF9 and a southwesterly wind occurred on UMD RF7. For all flights, the UMD aircraft departed from the Tipton airport (located between Washington, D.C. and Baltimore) and first flew a horizontal transect upwind of the study area to sample the incoming air. For the downwind transects of UMD-RF1–6 and RF8, an imaginary vertical plane AB was defined at the location where polluted plumes from the major emission sources—power plants, the I-95 highway, and the Washington, D.C., and Baltimore, MD metropolitan areas—could be sampled separately under northwesterly wind condition (see Figure 1). The aircraft made multiple horizontal transects at different altitudes in the plane AB to capture the outgoing air. Several vertical profiles were taken to measure vertical distribution of trace gases and to estimate the planetary boundary layer (PBL) height. For UMD-RF9, the sampling at downwind transects at various altitudes was conducted along the plane BC, since this flight was conducted under northeasterly winds. Data from UMD-RF7 are not used below because of the complex wind patterns prevalent in the study area on 24 February 2015.

The Purdue aircraft conducted a total of six research flights between 16 February to 11 March 2015 (Salmon et al., 2017; Salmon et al., 2018) (Figure 1 and S1). Purdue flight tracks were designed in a similar manner to the UMD flights, aiming to measure mole fractions of CO<sub>2</sub> upwind and downwind of the Balt-Wash area. On 19 February 2015 (Purdue-RF3), the Purdue aircraft was coordinated with the UMD aircraft (UMD-RF4) to

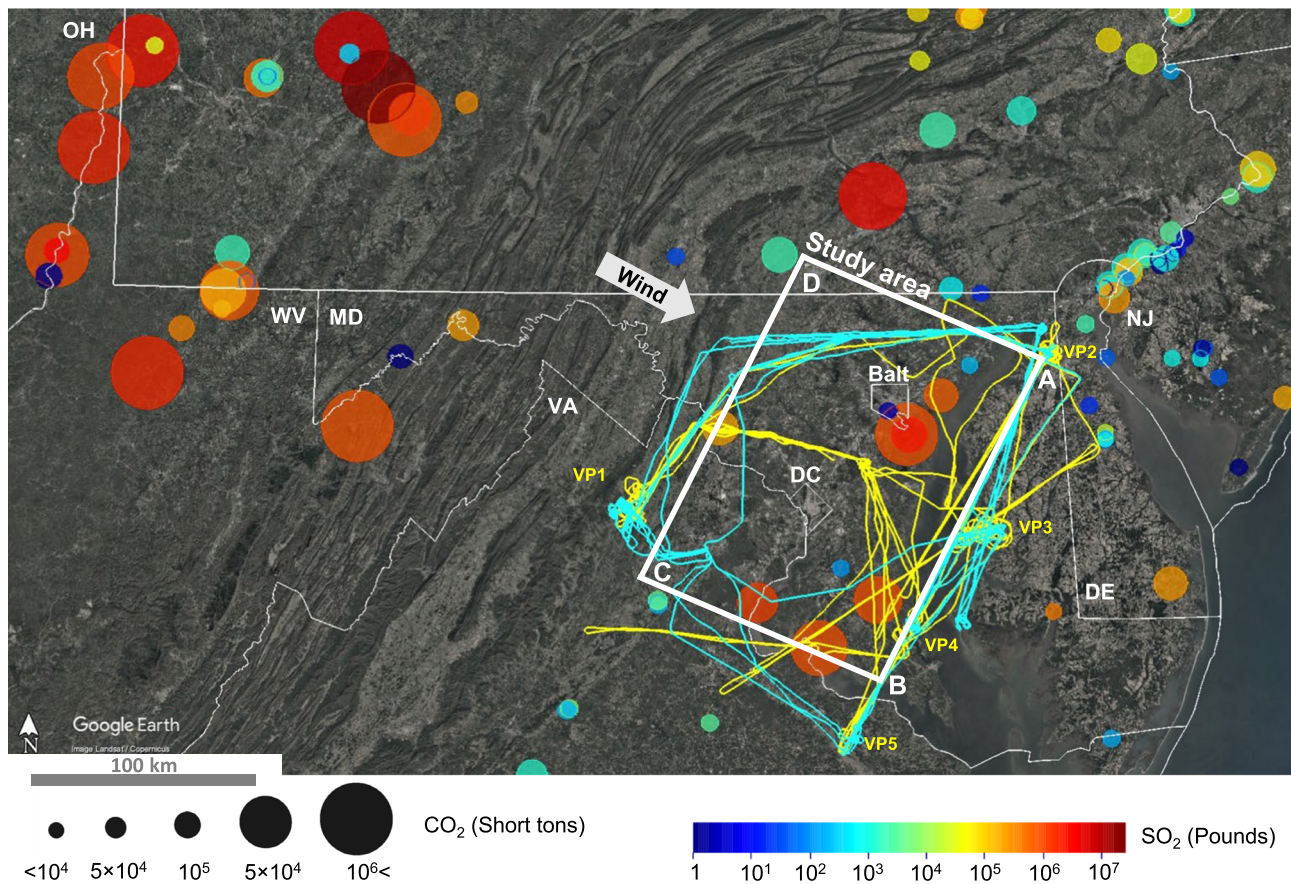


**Figure 1.** Overview of the FLAGG-MD aircraft campaign during February 2015 conducted in the Baltimore, MD and Washington, D.C. metropolitan areas; the white rectangle defines the Balt-Wash study area used throughout the analysis. Yellow and cyan lines indicate the UMD and Purdue aircraft flight tracks, respectively. The dominant wind direction during the campaign period is shown by the white arrow. Point emission sources are shown as circles; the size and color of these circles indicate the amount of CO<sub>2</sub> (size) and SO<sub>2</sub> (color) emitted from these sources in February 2015 (USEPA AMPD 2015). The VP labels indicate locations where vertical profile data were obtained. The points labeled A, B, C, and D denote the edge of the region for which the emission of CO<sub>2</sub> from the Balt-Wash region is found. The boundary of the vertical plane AB, for which transects at various altitudes were flown, is used to define the downwind study area to calculate the emission of CO<sub>2</sub> for all flights except UMD-RF9. The vertical plane BC is used to define the downwind boundary for UMD-RF9, since northeasterly winds were present on 26 February 2015.

conduct direct comparisons of in situ measurements of CO<sub>2</sub>, other GHGs, and meteorological variables during a wing-tip to wing-top segment that lasted about 40 min.

### 2.3. HYSPLIT Transport Modeling

In this study, the Hybrid Single Particle Lagrangian Integrated Trajectory (HYSPLIT) model was used to determine the sources of polluted plumes observed from the aircraft (Draxler & Hess, 1997; Stein et al., 2015). A series of back trajectories starting at the aircraft locations, at 1 s intervals, was computed using the default model configuration setup and NAM12 (North American Mesoscale Forecast System, 12 km horizontal resolution) as input meteorology. Forward transport modeling of power plant CO<sub>2</sub> plumes was conducted using HYSPLIT particle dispersion mode with NAM4 (4 km horizontal resolution). The number of particles released per cycle (variable name “numpar”) was set to  $10^6$ . The output mass was divided by air density to obtain mole fraction (ichem = 6). Horizontal grid spacing was specified as  $0.1^\circ$ , given that the objective of the modeling is to understand the inter-state transport of power plant plumes in the eastern U.S. vertical grid spacing was set at 100 m below 2,000 m and at 500 m above 2,000 m. All other configuration parameters were set at default values, as described in Draxler et al. (2014). As input emission sources, we used power plants listed in the Environmental Protection Agency’s Clean Air Markets Division (EPA CAMD) data sets for Washington, D.C., Maryland, Pennsylvania, Virginia, West Virginia, and Ohio.

The EPA CAMD emission data set of facility-level hourly CO<sub>2</sub> emissions records was obtained from the Air Markets Program Data (AMPD) query system (USEPA AMPD, 2015).

#### 2.4. VEGAS Modeling and NDVI Data

A VEgetation-Global Atmospheric-Soil (VEGAS) model simulation was used to calculate the biogenic flux of CO<sub>2</sub> over the Balt-Wash area during February 2015. VEGAS is a dynamic soil and vegetation model that simulates the growth of plant functional types based on meteorological data (Zeng et al., 2004, Zeng et al., 2005). The model was run hourly at 9 km resolution using re-gridded NARR (North American Regional Reanalysis) data as meteorological input. The simulation was started in the year 1715 to provide a spin-up time for regional carbon pools.

In addition to the benefit of estimating the biogenic CO<sub>2</sub> flux for the study domain, gridded VEGAS biogenic CO<sub>2</sub> flux output was combined with the normalized difference vegetation index (NDVI) data to investigate the impact of biogenic CO<sub>2</sub> emissions on the background CO<sub>2</sub> that is needed for the mass balance calculation (see section 3.5.1). Since the VEGAS model was not specifically designed to compute biogenic emissions of CO<sub>2</sub> in regions with complex landscapes such as the Balt-Wash study area, we have combined VEGAS output with NDVI data acquired within the study region during February 2015. First, gridded VEGAS output of net biogenic CO<sub>2</sub> flux was computed for the entire Balt-Wash study area. Next, version v1r12 NDVI data (4 km, weekly, <https://www.star.nesdis.noaa.gov/smcd/emb/vci/VH/index.php>) from the Visible Infrared Imaging Radiometer Suite (VIIRS) on the Suomi National polar-orbiting partnership (Suomi-NPP) was summed within each of the narrow grid boxes (NDVI<sup>GRID BOX</sup>) perpendicular to line AB as shown in Figure S2. Then, the horizontal transect of the biogenic flux of CO<sub>2</sub> within the study region, along line AB, was found by multiplying the VEGAS output (i.e., a single number representative of the entire study region) by the value of NDVI<sup>GRID BOX</sup> for each specific grid box and dividing by the sum of NDVI<sup>GRID BOX</sup> for all grid boxes. In section 3.5.1, we describe the impact of biogenic CO<sub>2</sub> flux on the background CO<sub>2</sub> and the mass balance calculation.

#### 2.5. Mass Balance Approach and Sensitivity Analysis

A mass balance approach was used to estimate the emission rate of CO<sub>2</sub> from the Balt-Wash area and from two local power plants. Under steady wind conditions, the horizontal flux of CO<sub>2</sub> crossing the vertical plane AB located downwind of an emission source can be considered as an approximation of the vertical flux of CO<sub>2</sub> over the emission source, while the air parcel was passing through the source (Trainer et al., 1995; White et al., 1983). A similar approach has been used in previous studies to estimate fluxes of trace gases such as CO<sub>2</sub>, CH<sub>4</sub>, CO, and NO<sub>x</sub> from various emission sources (Cambaliza et al., 2014; Heimbürger et al., 2017; Kalthoff et al., 2002; Karion et al., 2015; O'Shea et al., 2014; Peischl et al., 2016; Salmon et al., 2017; Salmon et al., 2018). In this study, the emission rate of CO<sub>2</sub> ( $F$ , mol s<sup>-1</sup>) was calculated with the following equation:

$$F = \int_{z_i}^{z_f} \int_{x_i}^{x_f} ([C]_{x,z} - [C_{bg}]_{x,z}) \cdot U_{x,z} \cdot k_x \, dx dz \quad (1)$$

where  $x$  is the horizontal and  $z$  is the vertical location in the plane AB. Variables  $x_i$ ,  $x_f$  and  $z_i$ ,  $z_f$  are the horizontal and vertical bounds of AB influenced by the emission source of interest,  $[C]$  is the sampled number density of CO<sub>2</sub>, and  $[C_{bg}]$  is the computed background number density of CO<sub>2</sub>. Also,  $U$  is the wind speed perpendicular to the aircraft heading and  $k$  is the scaling factor for  $U$ , defined as the ratio of the mean  $U$  during transport time over the emission source to the value of  $U$  measured at the downwind flights. A detailed description of each parameter is provided in the following sections.

##### 2.5.1. Background Mole Fractions of CO<sub>2</sub>

For the Balt-Wash area, background regions within the downwind transects were designated at northern and southern edges (Krautwurst et al., 2016). Then, the CO<sub>2</sub> background was defined by fitting a linear regression line to the mole fractions of CO<sub>2</sub> measured at both edges of the transects (Figure S3b, S3d, S3e, S3g). On 19 and 23 February 2015 the mole fractions of CO<sub>2</sub> measured between the Washington, D.C. and Baltimore, MD plumes along line AB in Figure 1 were lower than mole fractions of CO<sub>2</sub> measured at the edges of the downwind transect (Figure S3a, S3c, S3f). Our HYSPLIT transport modeling indicates that elevated CO<sub>2</sub> at the downwind transect edges on these dates was likely due to power plant plumes transported

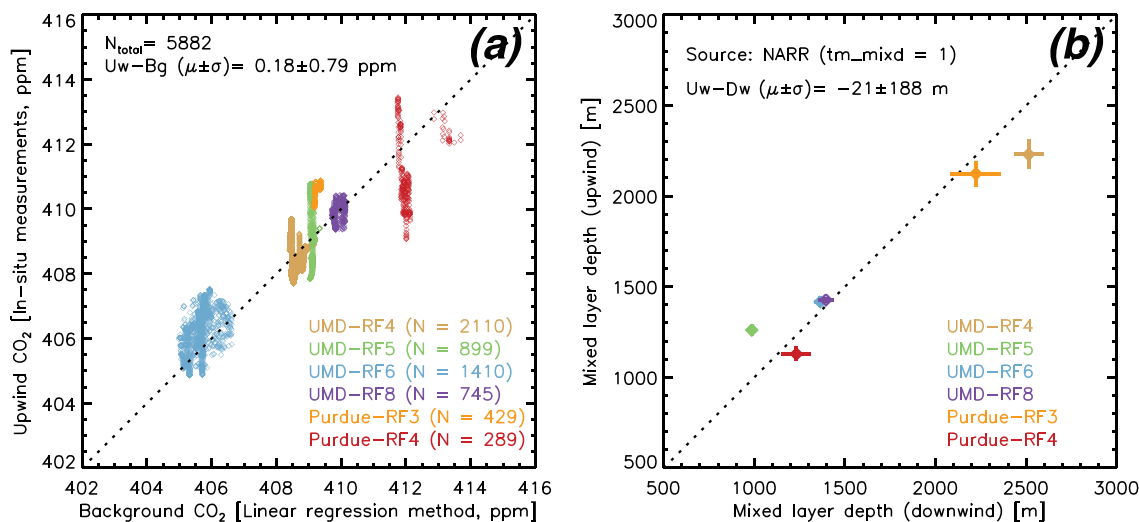


**Figure 2.** Scatter plot of the upwind CO<sub>2</sub> mole fraction (10 s running mean) versus the paired downwind, background estimate of CO<sub>2</sub>. The number of paired data points for each flight is indicated on panel (a); the total number of paired points (5,882) yields a mean and standard deviation of  $0.18 \pm 0.79$  ppm. Panel (b) shows the mixed layer depth extracted from HYSPLIT run using North American Regional Reanalysis (NARR) meteorological fields along the upwind aircraft flight track and the location of the paired, downwind data. Results are shown for six of the seven mass balance flights considered in the analysis, because upwind measurements of CO<sub>2</sub> were not obtained for UMD-RF9.

from either Pennsylvania or West Virginia (see section 3.2). Therefore, an additional background region, approximately midway between the Washington, D.C. and Baltimore, MD plumes, was designated for the flights conducted on 19 and 23 February 2015. For the three flights (UMD-RF4, UMD-RF6, and Purdue-RF3) conducted on these 2 days, background CO<sub>2</sub> was determined by fitting two linear regression lines: one from the southern edge to the midway background flight segment and another from the midway segment to the northern edge. The background mole fractions of CO<sub>2</sub> were converted into background number density ( $[C_{bg}]$ ) using in situ measurements of temperature and the pressure, for use in equation (1).

The accuracy of our estimate of the background CO<sub>2</sub> mole fraction was evaluated by conducting a comparison to upwind measurements of CO<sub>2</sub> (Figure 2). For the comparison, the CO<sub>2</sub> background value defined at each point of every downwind transect was examined for potential pairing to the upwind measurements of CO<sub>2</sub> conducted for the same flight. Forward HYSPLIT trajectories were computed every 1 s of each upwind flight segment, which generally occurred along the line CD in Figure 1. For each forward trajectory, a successful pairing was determined if a trajectory crossed the downwind transect meeting the following conditions: (1) trajectory altitude was within the PBL at the crossing time of the downwind track, and (2) the crossing time of the downwind track was within  $\pm 1$  hr of the time the aircraft collected data. The upwind data were collected in early afternoon for all of the flights, and the downwind sampling occurred on average 2.5 hr later. Figure 2a shows a comparison of a 10 s running mean of CO<sub>2</sub> within the PBL collected during the upwind portion of the indicated flights versus the background value of CO<sub>2</sub> computed for the location at which the trajectory crossed the downwind track. The excellent agreement between the upwind measurements of CO<sub>2</sub> and our estimate background CO<sub>2</sub> (mean and standard deviation of  $0.18 \pm 0.79$  ppm) supports the validity of the carbon emissions computed using the mass balance approach. We are unable to compare upwind CO<sub>2</sub> to the estimate of background for UMD-RF9, because the aircraft flight track did not sample the composition of the atmosphere along line AD in Figure 1 that corresponds to the upwind location for this flight, due to the presence of northeasterly winds.

Figure 2b compares the depth of the mixed layer, for the upwind flight leg (ordinate) and downwind flight leg (abscissa). The values originate from the North American Regional Reanalysis (NARR) meteorological fields for February 2015, because the depth of the PBL from NARR exhibits the closest agreement with the depth of the PBL inferred from our flight data. Figure 2 shows considerable variations in both the depth of the PBL and upwind CO<sub>2</sub>, between the six flights for which such a comparison is possible. Undoubtedly, this variation in the depth of the PBL plays a role in value of CO<sub>2</sub> along the upwind leg. The fact that the

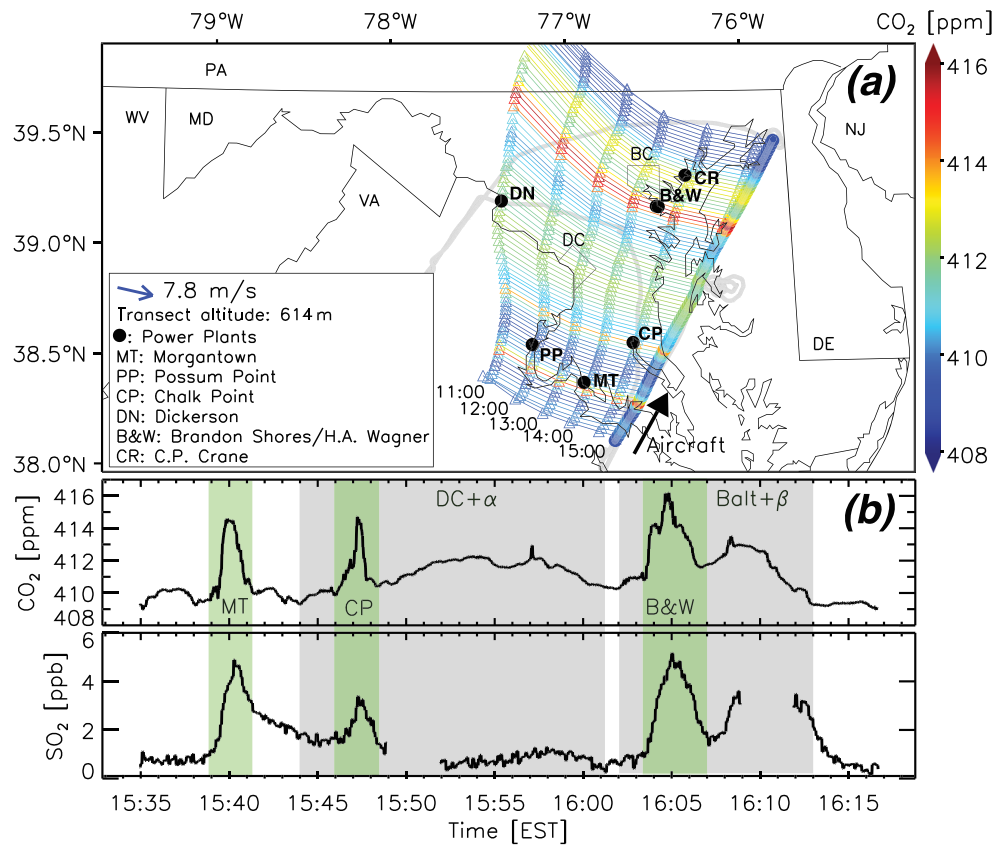


**Figure 3.** (a) Colored lines depict back trajectories initiated along the aircraft track, downwind of the Balt-Wash area on 20 February 2015 (UMD-RF5). Triangles indicate the locations of back trajectories at every hour. Black circles indicate the major power plants in the study area. Mean aircraft altitude and the wind speed and direction measured during the flight are shown in the left box. (b) Time series of mole fractions of CO<sub>2</sub> and SO<sub>2</sub> measured during the same flight track. Green shaded areas indicate the plumes partially attributed to local power plants while the gray shaded areas indicate urban plumes. The DC+ $\alpha$  label indicates that the plume is attributed to Washington, D.C. and nearby Dickerson power plant. The Balt+ $\beta$  label indicates that the plume is attributed to Baltimore, MD and to major power plants in Pennsylvania (labeled as PA in the map, see Figure 4 for further analysis). See section 3.5.1 for detailed spatial distribution of fossil-fuel CO<sub>2</sub> flux over the study area.

depth of the PBL is stable between the upwind and downwind portions of the flight again supports the validity of the carbon emissions found using our mass balance approach.

For power plant plumes, the horizontal bounds of the plume were determined based on large, sharp gradients in the in situ measurements of CO<sub>2</sub> as shown in Figure 3. The connection of these enhancements of CO<sub>2</sub> to local, nearby power plant emissions was confirmed based upon visual inspection of HYSPLIT back trajectories initialized every 1 s along the flight track, shown also in Figure 3. The CO<sub>2</sub> background for power plant plumes was defined as a linear function fit to the mole fractions of CO<sub>2</sub>, measured by the Picarro (G2401-m) on board the aircraft, at the either side of the plume's bounds. All 16 power plant plumes considered below displayed large enhancements of CO<sub>2</sub> that could clearly be traced to a local, nearby power plant.

### 2.5.2. Wind

Recently, a systematic aircraft heading-dependent bias was identified in wind speed and direction recorded by the Garmin system onboard the UMD aircraft (Ren et al., 2019). A series of bias correction methods was developed and applied to the wind measured by the UMD aircraft, utilizing a newly installed differential GPS instrument, NAM4 wind data, and local wind profilers. Text S1–S3 provide a detailed description on how the systematic bias in the aircraft wind measurements was corrected. The wind speed perpendicular to the aircraft heading ( $U$ ) was calculated using the wind speed, wind direction, and true track angle of the aircraft measured downwind of the emission source of interest. Then, 10 s running means of  $U$  were

**Table 1**

Summary of the Mass Balance Parameters Used to Estimate the Emissions of CO<sub>2</sub> From the Balt-Wash Area

	Date	$z_f \pm 1\sigma$ [m]	$[\text{CO}_2] \pm 1\sigma$ [ppm]	$[\text{CO}_{2,bg}] \pm 1\sigma$ [ppm]	$\bar{U} \pm 1\sigma$ [m s <sup>-1</sup> ]	$\bar{k} \pm 1\sigma$
UMD-RF4	19 February 2015	1,372 ± 280	409.3 ± 0.8	408.5 ± 0.3	12.8 ± 1.6	0.95 ± 0.01
UMD-RF5	20 February 2015	1,109 ± 139	411.2 ± 1.4	409.4 ± 0.2	5.6 ± 1.4	0.75 ± 0.04
UMD-RF6	23 February 2015	1,013 ± 265	406.8 ± 1.1	405.7 ± 0.4	10.6 ± 1.5	1.06 ± 0.01
UMD-RF8	25 February 2015	1,393 ± 137	410.1 ± 1.9	408.6 ± 0.9	5.3 ± 2.0	0.91 ± 0.05
UMD-RF9	26 February 2015	896 ± 268	417.9 ± 2.5	414.2 ± 0.8	3.9 ± 1.1	0.90 ± 0.04
Purdue-RF3	19 February 2015	1,372 ± 280	410.0 ± 0.5	409.2 ± 0.2	12.7 ± 1.3	1.00 ± 0.02
Purdue-RF4	27 February 2015	1,626 ± 349	414.3 ± 2.4	412.6 ± 0.6	5.1 ± 1.6	0.98 ± 0.04

Note. For the boundary layer height ( $z_f$ ), the best estimates and  $1\sigma$  uncertainties are shown. For the mole fraction of CO<sub>2</sub> ( $[\text{CO}_2]$ ), CO<sub>2</sub> background ( $[\text{CO}_{2,bg}]$ ), perpendicular wind speed ( $U$ ), and the wind variability during air transport across the study area ( $k$ ), the mean and the standard deviation during the downwind flight period are shown (see section 2.5). The flux of CO<sub>2</sub> was calculated for each point in each transect, and thus the mean  $[\text{CO}_2]$ ,  $[\text{CO}_{2,bg}]$ ,  $U$ , and  $k$  values thus not directly translate into the mass balance estimate results.

used for the mass balance calculation. For the sensitivity analysis, the standard deviation of  $U$  during the downwind transect period was added/subtracted from the original  $U$  for the mass balance calculation.

From back trajectory analysis of seven mass balance flights (UMD RF4,5,6,8,9, Purdue RF3,4), we found that the average air transport time over the Balt-Wash area was ~5 hr, given the average wind speed of ~7 m s<sup>-1</sup> across the study area. However, the value of  $U$  varies across the study area, which does have an impact on CO<sub>2</sub> emissions found using the mass balance approach. To account for the variability of  $U$  during the transport time of air across the study area, a scaling factor  $k$  was estimated in following manner. For each 0.1° × 0.1° horizontal grid, average  $U$  within the PBL (hereafter  $\bar{U}_{PBL}$ ) was derived from NAM4 for the hour closest to the mean aircraft observation time (Figure S4a). Then, the resulting values of  $\bar{U}_{PBL}$  were averaged within a series of diagonal latitudinal bins across the Balt-Wash study area (Figure S4b). For each latitudinal bin, the scaling factor  $k$  was calculated by dividing the mean of all  $\bar{U}_{PBL}$  with the  $\bar{U}_{PBL}$  at the downwind edge. Obtained  $k$  for latitudinal bins were interpolated and applied to individual wind measurements ( $U$ ) (Figure S4c). We found that  $k$  values averaged for each of the seven mass balance flights range from 0.75 to 1.06 (Table 1). For the sensitivity analysis,  $k$  was calculated using the same method, but for ±1 hr from the mean aircraft observation time. Then, the standard deviation of  $k$  within 3 hr span was added/subtracted from the original  $k$  for the mass balance calculation.

To address the impact of the scaling factor  $k$  on our determination of emissions of CO<sub>2</sub> from the Balt-Wash area, emissions were also estimated assuming consistent perpendicular wind speed throughout the transport time ( $k = 1$ ). When consistent wind ( $k = 1$ ) is assumed, the monthly total FFCO<sub>2</sub> emission was estimated to be 2.0 MtC, which is 5% larger than the estimate of 1.9 MtC that accounts for the variability of  $U$  during the air transport time. Further details are given in Figures S5 and S6. Given the relatively short transport time of power plant plumes between emission and aircraft sampling, the scaling factor  $k = 1$  was used for the calculation of power plant emissions of CO<sub>2</sub>.

### 2.5.3. Vertical and Horizontal Boundary

To include emissions of CO<sub>2</sub> transported above the PBL into our estimate of CO<sub>2</sub> emissions, the adjusted mixing height ( $z_{adj}$ ) was determined and used as a vertical bound ( $z_f$ ) of the mass balance equation. First, the well-mixed PBL height ( $z_{pbl}$ , dashed line in Figure S7) and the entrainment height ( $z_e$ , dotted line in Figure S7), an altitude where mixing from the PBL has reached free tropospheric level, were determined from the vertical profiles of potential temperature and mole fractions of the trace gases (CO<sub>2</sub>, CH<sub>4</sub>, and H<sub>2</sub>O). Then, the adjusted mixing height ( $z_{adj}$ ) was calculated using  $z_{adj} = (3z_{pbl} + z_e)/4$ , as described by Peischl et al. (2016). Also, ±1σ uncertainty of  $z_{adj}$  was determined as  $\pm(z_{pbl} - z_e)/2$  (Figure S7), again from Peischl et al. (2016). For flights that obtained multiple vertical profiles (UMD-RF4,5,8 and Purdue-RF3,4), the adjusted mixing height and its uncertainty ( $z_{adj} \pm 1\sigma$ ) determined from each vertical profile were linearly fit as a function of the observation time. From this function, the vertical boundary of the PBL and its uncertainty ( $z_f \pm 1\sigma$ ) were determined at the mid-point of the downwind flight period. For the flights with a single vertical profile in the downwind region (UMD-RF6,9), values of  $z_{adj}$  and their 1σ estimated from the only



vertical profile were used to define  $z_f \pm 1\sigma$ . For the sensitivity analysis, values of  $z_f \pm 1\sigma$  were used as the vertical boundary in the mass balance calculation.

Horizontal boundaries ( $x_i$ ,  $x_f$ ) were determined as the locations where the HYSPLIT back trajectory passed through the southern and northern bounds of the Balt-Wash area (UMD-RF4,5,6,8 and Purdue-RF3,4). For UMD-RF9, horizontal boundaries were determined as the locations where the back trajectory went through the western or southern bound of the study area. To estimate the emission rate of CO<sub>2</sub>, horizontal fluxes were calculated for each point in the downwind transects (unit: gC m<sup>-2</sup> s<sup>-1</sup>). The calculated fluxes were averaged into a single value, then multiplied by the horizontal ( $x_f - x_i$ ) and vertical boundary distances ( $z_f - z_i$ ) (unit: gC s<sup>-1</sup>), as described by equation (1).

### 3. Results

#### 3.1. Source Identification and Attribution: Baltimore, MD-Washington, D.C. Area

During the aircraft campaign, spikes of CO<sub>2</sub> were often observed. For example, for UMD-RF5 on 20 February 2015, three spikes of CO<sub>2</sub> were recorded downwind of the Balt-Wash area (green shaded areas in Figure 3b). To determine the sources of these plumes, a series of HYSPLIT back trajectories were calculated. When the wind direction was consistent during the transport over the Balt-Wash area, which was the case for 20 February 2015, power plant plumes could be clearly isolated from the emissions of the surrounding urban region (Figure 3a). The first two spikes of CO<sub>2</sub> observed at 15:40 and 15:47 (EST) were attributed to the Morgantown (MT) and Chalk Point (CP) power plants, respectively. The spike of CO<sub>2</sub> observed downwind of the Baltimore, MD (16:05) was attributed to the Brandon Shores and H. A. Wagner (B&W) power plants, which are in close proximity. According to CEMS records, the B&W, MT, CP power plants emitted 1470, 980, 540 tons of CO<sub>2</sub> and 2.8, 0.8, 0.8 tons of SO<sub>2</sub>, respectively, during a 1-hr period from 14:00 p.m. to 15:00 p.m. on 20 February 2015. Simultaneous increases of the mole fractions of SO<sub>2</sub> for the three spikes of CO<sub>2</sub>, showing ratios of SO<sub>2</sub>/CO<sub>2</sub> mole fraction similar to those from CEMS records, confirm that the plumes were emitted from power plants. The B&W, MT, and CP power plants emitted total of 3.4 MtC in year 2015, contributing 75.4% of the annual total power plant emissions of CO<sub>2</sub> in Maryland (USEPA GHGRP, 2019).

Along with the three spikes of CO<sub>2</sub> attributed to local power plants, broad areas of increased CO<sub>2</sub> were observed downwind of the Washington, D.C. and Baltimore, MD (gray shaded areas in Figure 3b). We argue that increased mole fractions of CO<sub>2</sub> downwind of the Washington, D.C. area were mostly induced by emissions from local fossil fuel combustion, while increased CO<sub>2</sub> downwind of Baltimore was induced by a mixture of plumes from that city and from several power plants in the state of Pennsylvania (see section 3.2).

#### 3.2. Source Identification and Attribution: Inter-State Transport of Power Plant Plumes

During the aircraft campaign, several spikes in the mole fraction of SO<sub>2</sub> were observed both upwind and downwind of the Balt-Wash area. To find the sources of these plumes of SO<sub>2</sub>, HYSPLIT back trajectories were calculated on 6 days (Figures 4a–4f). These trajectories showed that some of the SO<sub>2</sub> plumes observed downwind of the Balt-Wash area are likely to be the same plumes observed on the upwind flight legs (Figures 4a, 4b, 4d, 4e). During UMD-RF8, the aircraft observed a broad increase of SO<sub>2</sub> north of Washington, D.C. due to advection from the westerly wind direction (Figure 4f). Figure 4g shows that several plumes of SO<sub>2</sub> observed downwind of the Balt-Wash area were transported from the mid-west Pennsylvania area where five large power plants are located. The total nameplate capacity of the five power plants was 6,444 MW (Coal: 90.3% Natural gas: 9.4%) according to USEIA (2016). The Homer City power plant was reported as one of the largest SO<sub>2</sub> emitting facility in the entire U.S. for 2015 (USEPA AMPD, 2015). As the five power plants are geographically aligned from northwest to southeast in close proximity, a northwesterly wind is likely to merge the plumes from these power plants, leading to the inter-state transport of a highly polluted plume with relatively small horizontal width into the Balt-Wash area.

To further investigate the impact of upwind power plant plumes on the aircraft measurements, forward transport modeling of power plant CO<sub>2</sub> was conducted for 19 and 20 February 2015 (UMD-RF4, 5). Figure 5 shows that airborne observations of the spikes in CO<sub>2</sub>, induced by both local and upwind power plants, were well reproduced by the forward modeling (HYSPLIT CO<sub>2</sub>). A contour map of HYSPLIT CO<sub>2</sub> shows that continuous flow of CO<sub>2</sub> from power plants in Pennsylvania (PA) and West Virginia (WV)

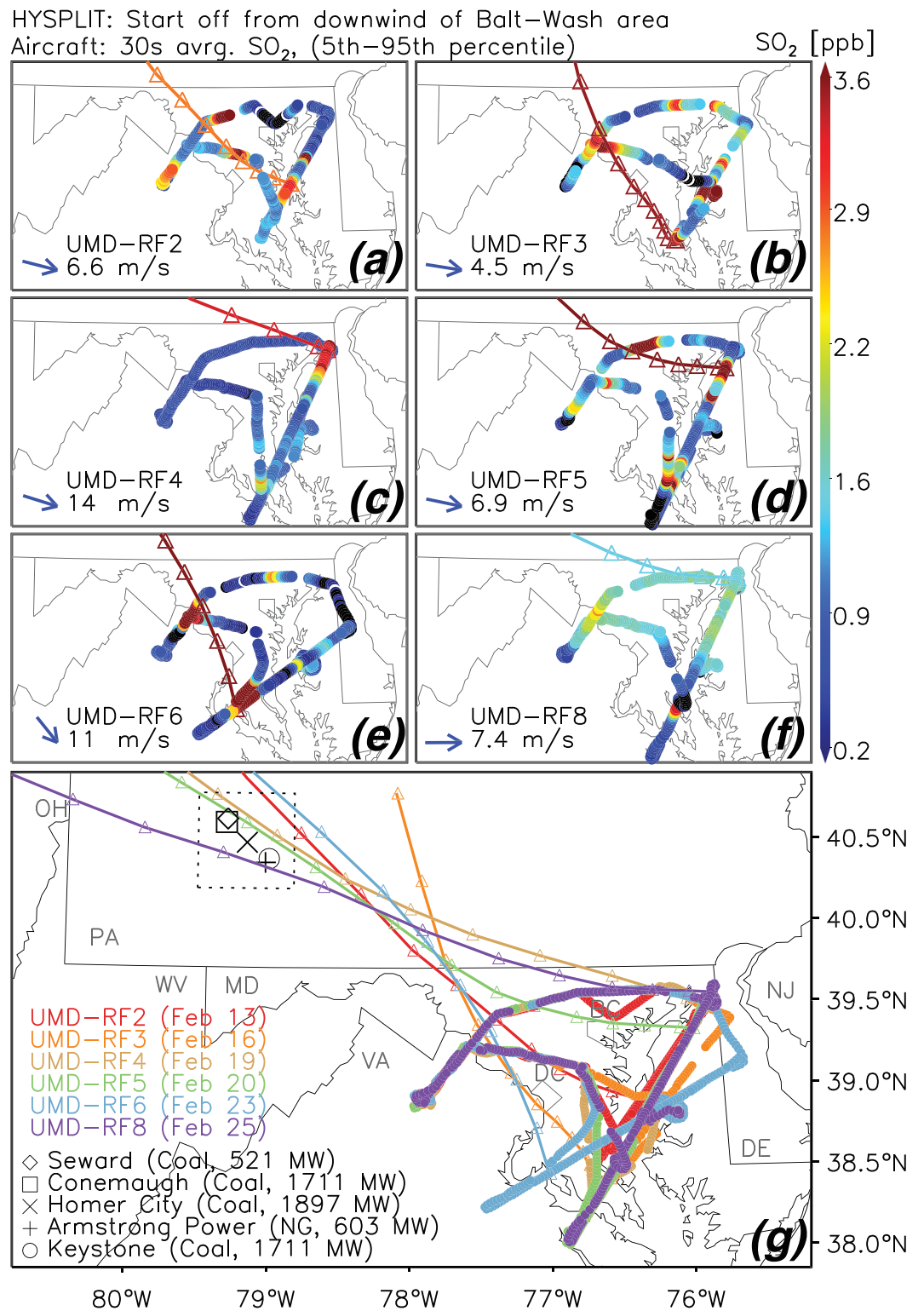


**Figure 4.** (a–f) Colored circles show mole fractions of SO<sub>2</sub> measured during six flights in February 2015. Colored lines are back trajectories initiated at the location of the SO<sub>2</sub> plume observed downwind of the Balt–wash area. Triangles on each trajectory show the location at every hour. Mean wind measured during the downwind flight is shown at the left–bottom corner of each panel. (g) A map showing same flight tracks and trajectories of (a–f) in a larger domain. The dashed box encloses the locations of five major power plants in Pennsylvania. The names of power plants, fuel, and their nameplate capacity are shown at the left–bottom corner (source: USEIA, 2016).

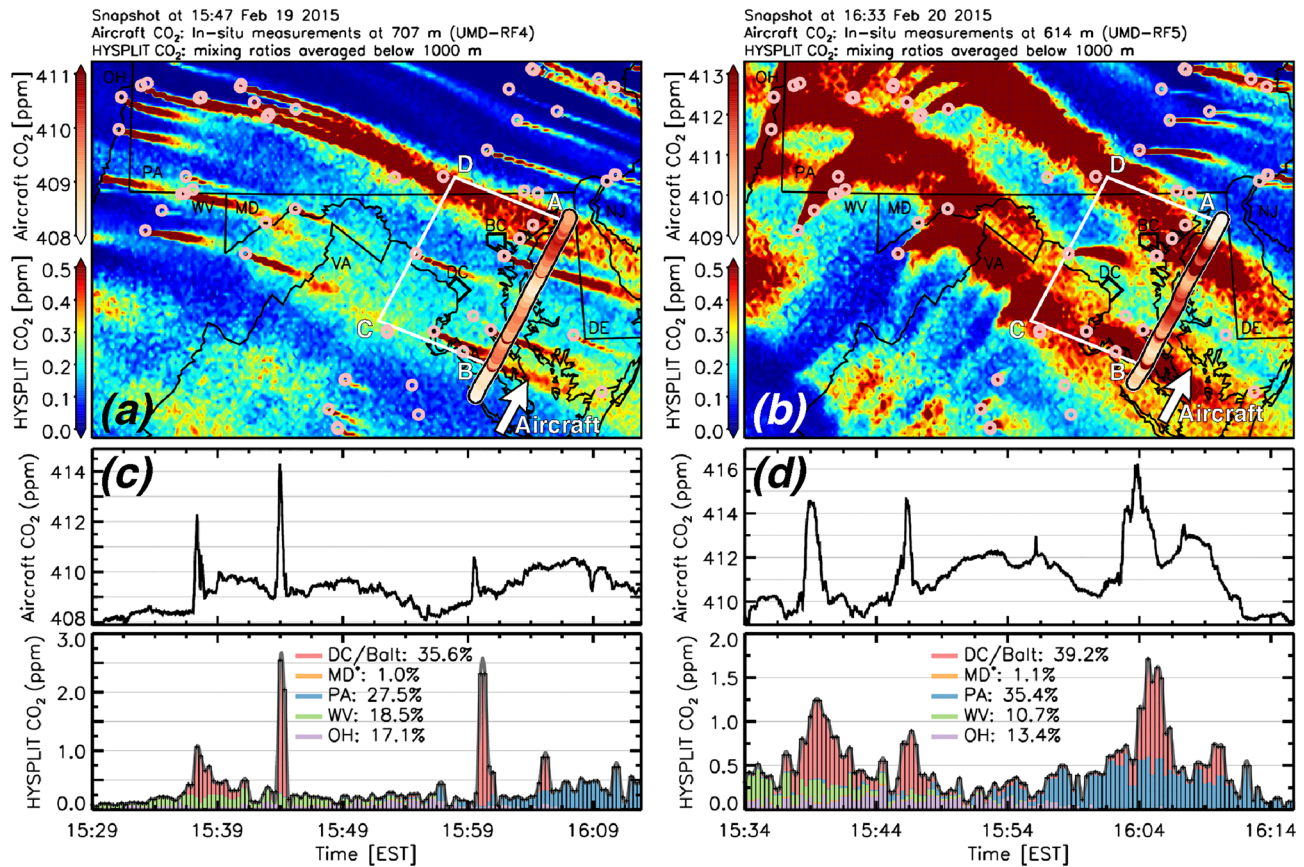


**Figure 5.** Maps showing HYSPLIT particle dispersion simulations of power plant emissions of CO<sub>2</sub> and flight tracks of (a) UMD-RF4 and (b) UMD-RF5. “HYSPLIT CO<sub>2</sub>” labels (color bars and y axes) indicate the enhancement of CO<sub>2</sub> due to power plant emissions averaged within the boundary layer. “Aircraft CO<sub>2</sub>” labels indicate measured mole fractions of CO<sub>2</sub> for a single transect, along the line A at 707 m (UMD-RF4) and 614 m (UMD-RF5) altitude. The location of power plant point emission sources used for the modeling are shown as pink circles. (c, d) Time series of “Aircraft CO<sub>2</sub>” at 707 m (UMD-RF4) and 614 m (UMD-RF5) altitude along the line AB and stacked bar plots of “HYSPLIT CO<sub>2</sub>” that were sampled for aircraft locations of the in-situ data. Each color of the bar indicates the state or region where the sampled HYSPLIT CO<sub>2</sub> was emitted; that is, emissions from the study area are denoted as DC/Balt. MD\* indicates the state of Maryland area outside DC/Balt box. The percentage of power plant emissions from region, for the given transects, is also provided (numbers sum to 100%).

sometimes passed through parts of the Balt-Wash area. According to the HYSPLIT analysis, CO<sub>2</sub> from power plants in PA passed downwind of Baltimore, MD and accounted for a significant portion of the total amount of CO<sub>2</sub> in the model grids (27.5% on UMD-RF4 and 35.4% on UMD-RF5). This forward modeling result agrees with the result from the SO<sub>2</sub> back trajectory analysis, which attributed some plumes of SO<sub>2</sub> observed downwind of Baltimore, MD to the power plants in PA (Figures 4c and 4d). However, CO<sub>2</sub> emitted by power plants in Ohio (OH) was relatively well distributed over a large horizontal distance when it reached the Balt-Wash area. This result implies that power plant emissions from OH and farther upwind states would have negligible impact on mass balance calculation for the Balt-Wash area. The emissions of CO<sub>2</sub> from power plants in PA and WV, however, must be considered in our analysis.

In summary, both the SO<sub>2</sub> back trajectory and CO<sub>2</sub> forward modeling results indicate that inter-state transport of power plant plumes can induce local increases of the mole fractions of CO<sub>2</sub> around the Balt-Wash area, especially when consistent northwesterly wind prevails. Accurate representation of the spatially varying CO<sub>2</sub> background is therefore needed to account for upwind power plant emissions of CO<sub>2</sub> in the mass flux calculation for the Balt-Wash area.

### 3.3. Power Plant Emissions: Evaluating the Aircraft-Based Mass Balance Approach

Prior to applying the mass balance approach to the Balt-Wash area, the accuracy and precision of the technique was evaluated using the CEMS records for CO<sub>2</sub> from two local power plants. Several spikes of

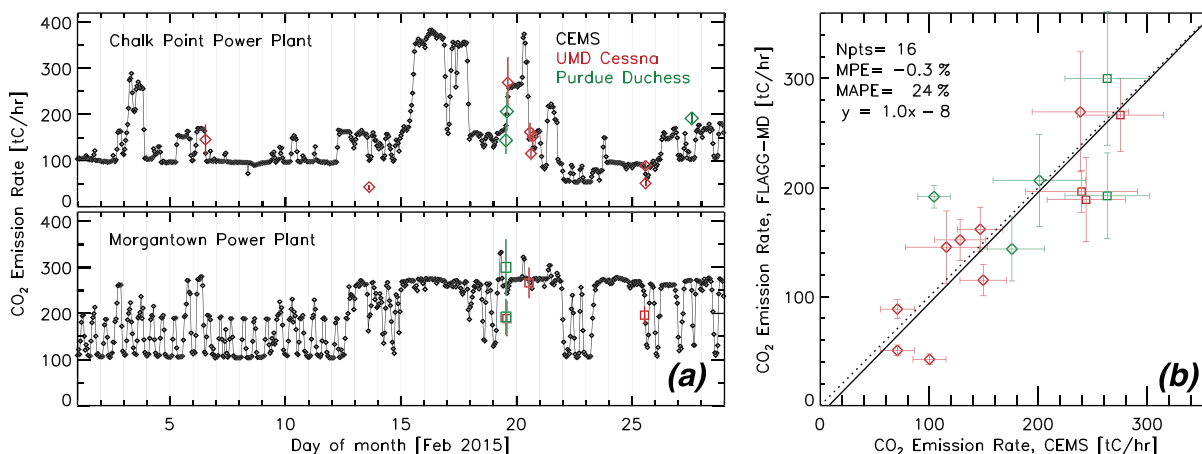


**Figure 6.** (a) Emission of CO<sub>2</sub> from the chalk point and Morgantown power plants in units of metric tons of carbon per hour. Black lines indicate the reported CEMS emission rates. Red and green diamonds represent the emission rates that we estimated using in situ measurements from the UMD and Purdue aircraft, respectively. (b) Scatter plot showing the comparison of the same dataset in (a). Dotted and solid lines indicate 1 to 1 ratio and linear regression lines, respectively. Vertical error bars on each diamond indicate the 1 $\sigma$  uncertainty induced by the uncertainty in the adjusted mixing height ( $z_{adj}$ ) (section 2.5.3). Horizontal error bars indicate the combined uncertainty of the CEMS records and the plume transport time (see Text S4).

CO<sub>2</sub> could be attributed to either the CP or MT power plant (Figure 3), and were used for the mass balance calculation. The total uncertainty of the CEMS records was determined by propagating individual uncertainty in the following terms: volumetric flow rate/CO<sub>2</sub> concentration measurements by CEMS (USEPA, 2009), difference of CEMS records against fuel consumption based U.S. Energy Information Administration (EIA) data sets (Gurney et al., 2016; Quick & Marland, 2019), and atmospheric transport time of power plant plumes. A detailed description of this uncertainty propagation is given in Text S4.

In Figure 6a, colored symbols show the 16 aircraft-based mass balance estimates of emission rates of CO<sub>2</sub> for the CP and MT power plants. The black lines show the hourly emission record of each power plant reported to EPA CAMD. According to EPA CAMD, a total of 0.23 MtC was emitted by the two power plants during February 2015. Of the total emissions, 98.8% was measured directly by CEMS, while 1.2% was either calculated or went through substitution procedures. All emissions records during the mass balance flights period were solely from CEMS.

The mean percentage error (MPE) and the mean absolute percentage error (MAPE) were -0.3% and 24%, respectively, for all 16 mass balance estimates the CO<sub>2</sub> emission rate (FLAGG-MD) relative to that provided by CEMS (Figure 6b). The mean and standard deviation of the difference between the FLAGG-MD and CEMS emission values are  $-5 \pm 43$  tC/hr. However, much larger differences, ranging from -58% to 84%, are observed for individual plume sampling comparisons. The large variation in these individual relative differences implies that the emission rate of CO<sub>2</sub> estimated from a single mass balance experiment may include significant random error. Such random error is most likely to be induced by incomplete mixing of power plant plumes within the boundary layer, causing the unrepresentative sampling of power plant plumes. The CO<sub>2</sub> background, often considered as a significant source of uncertainty in the mass balance approach for urban plumes (Cambaliza et al., 2014; Heimburger et al., 2017; Turnbull et al., 2018), is unlikely to be a source of error for power plant plumes given their narrow horizontal widths and a large value of the term  $([C] - [C_{bg}])$  that appears in equation (1) (Figure 3). The mean value of  $([C] - [C_{bg}])$  at the peak of the spikes for the 16 sampled plumes was  $\sim 5.5$  ppm. We also found that the combined error for multiple mass balance estimates of power plant emissions decreases approximately as the square root of the number of the plume crossings rises, which suggests the estimates are indeed influenced by random error. Our analysis suggests that power plants emissions can be estimated with MPE of  $\sim 10\%$  (or less) when the total number of 12 (or more) plumes were sampled by aircraft for the mass balance calculation (95% confidence level). The importance of repeating mass balance experiments for the same emission source has been discussed in Heimburger et al. (2017).

**Table 2**  
*Sensitivity Test for the Aircraft-Based Mass Balance Estimates of the Emission of CO<sub>2</sub> From the Balt-Wash Area*

	UMD					Purdue		Mean
	RF4 19 February	RF5 20 February	RF6 23 February	RF8 25 February	RF9 26 February	RF3 19 February	RF4 27 February	
Baseline estimates [ $10^5 \text{ mol s}^{-1}$ ]	1.10	0.68	0.98	0.79	0.74	1.09	0.89	$0.89 \pm 0.15$
Relative Differences (RD) [%]								
Wind variability, Downwind	$\pm 13$	$\pm 25$	$\pm 14$	$\pm 39$	$\pm 29$	$\pm 18$	$\pm 39$	$\pm 25$
PBL height	$\pm 20$	$\pm 13$	$\pm 27$	$\pm 10$	$\pm 30$	$\pm 20$	$\pm 21$	$\pm 20$
CO <sub>2</sub> background	$\pm 19$	$\pm 11$	$\pm 16$	$\pm 9$	$\pm 19$	$\pm 18$	$\pm 20$	$\pm 16$
Instruments (Temp, Pres, CO <sub>2</sub> )	$\pm 8$	$\pm 3$	$\pm 6$	$\pm 4$	$\pm 2$	$\pm 11$	$\pm 5$	$\pm 5$
Wind variability, Transport	$\pm 1$	$\pm 4$	$\pm 1$	$\pm 4$	$\pm 6$	$\pm 2$	$\pm 3$	$\pm 3$
Total uncertainty [RSD, %]	$\pm 32$	$\pm 31$	$\pm 34$	$\pm 41$	$\pm 49$	$\pm 33$	$\pm 49$	$\pm 38$

*Note.* Baseline estimates from the seven flights are shown on the first row. Relative differences indicate the changes of the baseline estimate when the  $\pm 1\sigma$  uncertainty of each mass balance parameter is used to calculate the emission of CO<sub>2</sub>. The total  $1\sigma$  uncertainty of each baseline estimate is shown as the relative standard deviation (RSD) at the bottom row. On the column labeled “Mean,” the mean and SEM95 values of seven Baseline estimates were shown in the first row, and the mean values were shown for the remaining rows.

### 3.4. The Baltimore, MD-Washington, D.C. Area Emissions: Sensitivity Analysis

The emission rate of CO<sub>2</sub> from the Balt-Wash area was estimated based on the five UMD flights and two Purdue flights. Table 1 summarizes the mean and the standard deviation of the five mass balance parameters shown in equation (1) for these seven flights.

Table 2 shows the baseline estimates of the emission rate of CO<sub>2</sub> that we consider to be the best estimates for the seven research flights. As the experimental period spans 9 days in late February, the emission rate of CO<sub>2</sub> from the study area may be assumed to be constant during the sampling period. This assumption is supported by the fact that the emission rate of CO<sub>2</sub> derived from FFDAS shows small variation during the sampling period, having a relative standard deviation of 3% (see section 3.5.2). Assuming a constant emission rate, the standard error of the mean at 95% confidence level (SEM95) can be calculated as a measure of the precision with the following equation:  $\frac{t^* \sigma}{\sqrt{n}}$ , where  $t$ -Student = 2.306,  $\sigma$  is the sample standard deviation of the seven mass balance estimates and  $n$  is the number of the mass balance experiments (Heimburger et al., 2017). The mean of the seven baseline estimates and its SEM95 were  $89,000 \pm 15,000 \text{ mol s}^{-1}$  ( $3,870 \pm 630 \text{ tC/hr}$ ). This result indicates that the emission rate of CO<sub>2</sub> over the Balt-Wash area in the late February could be determined with the precision of 16% at 95% CL by repeating the mass balance experiments seven times within a 9 day span.

The sensitivity of the baseline estimates was tested against the following five parameters: background CO<sub>2</sub>, PBL height, wind variability observed during the downwind flight, wind variability during air transport cross the study area, and instrument uncertainty. For the sensitivity test, the  $\pm 1\sigma$  uncertainty value of each parameter were used for the mass balance calculation. Section 2.5 describes how the  $1\sigma$  uncertainty was determined for each of these five parameters. Table 2 shows relative differences (RD) of the newly calculated emission rates against their baseline estimates.

On average, the estimated emission rate of CO<sub>2</sub> is most sensitive to the uncertainty of the perpendicular wind speed observed during downwind flight, with the mean of the seven RD as  $\pm 25\%$ . The PBL height and the CO<sub>2</sub> background were the second and the third most important parameters contributing to the overall uncertainty in the emission rate of CO<sub>2</sub>. Instrument measurement uncertainties (temperature, pressure and CO<sub>2</sub>) and the wind variability during the air transport over the Balt-Wash area (parameter  $k$ ) show less significant impact the emission estimate of CO<sub>2</sub> than other parameters.

The total uncertainty ( $1\sigma$ ) for each baseline estimate was determined by propagating  $1\sigma$  values of the five sensitivity parameters using Monte Carlo simulations. The total uncertainty of seven mass balance estimates ranged from  $\pm 31\%$  to  $\pm 49\%$ , with the mean of the seven total uncertainties being  $\pm 38\%$ . The precision assigned to the mean of the seven independent mass balance estimates with SEM95 is  $\pm 16\%$ , which is much lower than the average of the seven total uncertainties (38%). These results are comparable to findings from

previous INFLUX studies that made use of an aircraft-based mass balance approach to estimate urban CO<sub>2</sub> emissions. Cambaliza et al. (2014) assigned an overall uncertainty of ~37% (or conservative ~50% when including unknown systematic errors) to the CO<sub>2</sub> emission rate estimated from a single aircraft-based mass balance experiment. Heimbürger et al. (2017) estimated CO<sub>2</sub> emission rates for the city of Indianapolis with SEM95 of ±17% by averaging nine aircraft-based mass balance estimates conducted during November–December 2014.

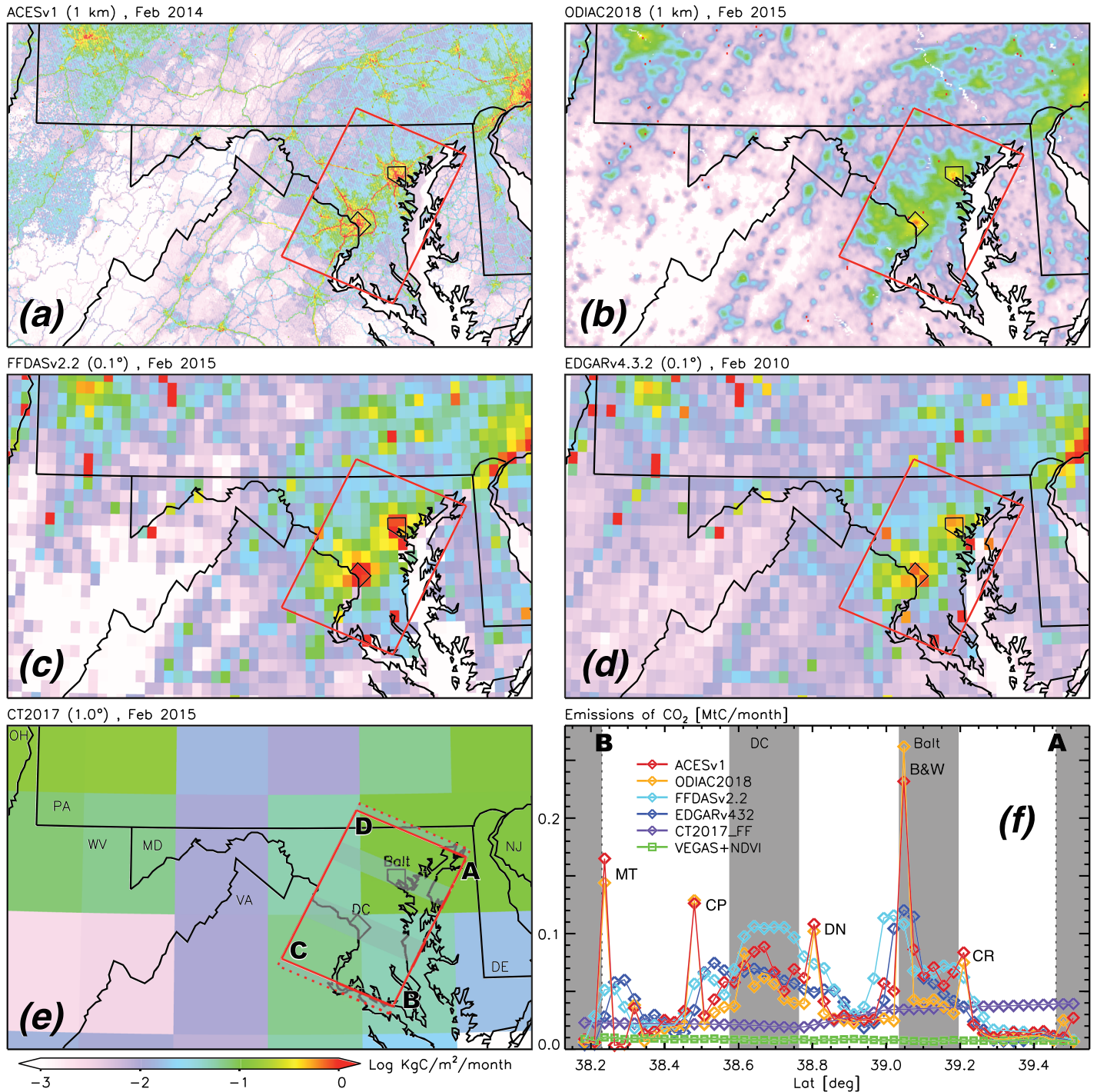
### 3.5. Comparison of Top-Down and Bottom-Up Emissions

In this study, differences between atmospheric observation based (top-down) and inventory data based (bottom-up) approaches were studied from three different perspectives. First, geographical distributions of CO<sub>2</sub> flux were compared for five bottom-up products: Anthropogenic Carbon Emissions System version 1 (ACESv1, Gately & Hutyra, 2017, 2018), Emissions Database for Global Atmospheric Research version 4.3.2 (EDGARv432, Janssens-Maenhout et al., 2017), FFDASv2.2, the Open-Source Data Inventory for Anthropogenic CO<sub>2</sub> version 2018 (ODIAC2018, Oda et al., 2018; Oda & Maksyutov, 2011, 2015), and CarbonTracker version 2017 (CT2017, Peters et al., 2007). Second, hourly emissions of CO<sub>2</sub> estimated from the aircraft (FLAGG-MD) were compared to hourly emissions from Fossil Fuel Data Assimilation System version 2.2 (FFDASv2.2, Asefi-Najafabady et al., 2014; Rayner et al., 2010). Finally, monthly emissions of CO<sub>2</sub> estimated from FLAGG-MD were compared to monthly emissions from the bottom-up products.

The bottom-up gridded products were largely developed based upon the emission downscaling method, which attempts to downscale national (or sub-national) and annual (or sub-annual) emissions inventories into model grids using spatiotemporal metrics (Gurney et al., 2019; Oda et al., 2019). For example, ODIAC2018 downscales emissions estimates from the Carbon Dioxide Information Analysis Center (CDIAC) into a 1 km global grid, using the carbon monitoring action (CARMA) data for power plants and the Defense Meteorological Satellite Program (DMSP) nightlight imagery for non-point sources. FFDASv2.2 downscales national emissions estimates by the International Energy Agency (IEA) onto a 0.1° resolution lat/lon global grid, using data assimilation to combine DMSP nightlight, population, traffic pattern, and power plant data. EDGARv432 downscales national sectoral emissions estimates onto a 0.1° lat/lon global grid for each emissions sector specified by IPCC. ACESv1 downscales the sector-specific emissions estimates provided by the National Emissions Inventory (NEI), Greenhouse Gas Reporting Program (GHGRP), and Database of Road Transportation Emissions (DARTE) onto 1 km spatial resolution U.S. northeast regional grid. CT2017 is a data assimilation system with four sectors: fossil fuel combustion, biosphere, ocean, and fire. For the biosphere and ocean sectors, prior model CO<sub>2</sub> fluxes were optimized onto a 1° lat/lon global grid using atmospheric CO<sub>2</sub> observations and transport simulations. For the fossil fuel combustion sector, emissions from ODIAC and the “Miller” emissions data set were averaged onto a 1° lat/lon global grid. The net amount of biogenic CO<sub>2</sub> emitted from the Balt-Wash area during February 2015 was computed from CT2017, and this value was compared to the VEGAS estimate of the biogenic CO<sub>2</sub> emissions (section 3.5.3).

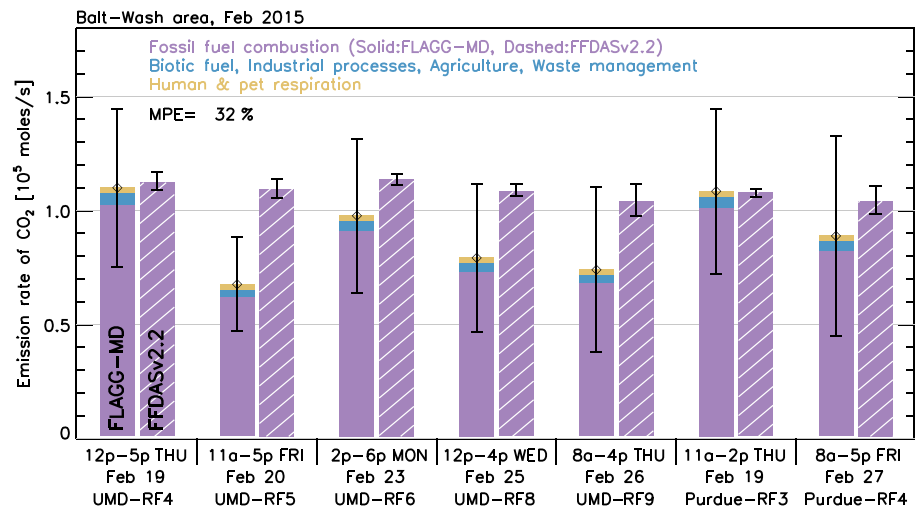
#### 3.5.1. The Baltimore, MD-Washington, D.C. Area: Spatial Distribution of CO<sub>2</sub> Flux

Figure 7 shows the spatial distribution of Fossil Fuel CO<sub>2</sub> (FFCO<sub>2</sub>) flux over the Balt-Wash area from the five bottom-up products. These five bottom-up emission inventories indicate similar overall patterns but distinctly different geographic distributions of the emissions due to variations in the underlying metrics that drive the emissions as well as spatial resolution. ACESv1 (with a 1 km resolution) shows highly resolved geographical distributions of FFCO<sub>2</sub>, such as the Beltway around Washington, D.C. and I-95 highway connecting major cities in the northeast corridor, due to their use of census block-level geospatial information (Gately & Hutyra, 2017). ODIAC2018, also at 1 km resolution, does not resolve individual roads due to their use of satellite-observed nighttime light data as a spatial emission proxy for non-point source emissions (Oda et al., 2018; Oda & Maksyutov, 2011). Still, it is noticeable that the global model ODIAC2018 shows a horizontal transect of CO<sub>2</sub> flux summed across the study area that is similar to that from the regional model ACESv1 (Figure 7f). The difference between ACESv1 and ODIAC2018 emissions would be less significant at an aggregated coarser spatial resolution, such as the resolution of the many inverse model simulations (Oda et al., 2019). Maps of CO<sub>2</sub> flux from FFDASv2.2 and EDGARv432 (0.1° resolution) show emission hot spots for the major power plants and the urban areas. Emissions from these power plants are represented by the higher resolution ACESv1 and ODIAC2018 inventories but are difficult to see on panels (a) and (b) of



**Figure 7.** Maps of FFCO<sub>2</sub> flux over the mid-Atlantic region from (a) ACESv1, (b) ODIAC2018, (c) FFDASv2.2, (d) EDGARv432, (e) CT2017. The Balt-Wash study area is indicated as a red box. (f) Horizontal transects of CO<sub>2</sub> flux derived from the biogenic model (VEGAS+NDVI) and the five FFCO<sub>2</sub> products (unit: million tons carbon (MtC) per month). These transects were obtained by summing the flux along diagonal latitudinal bins, as indicated by four gray shaded areas shown in panel (e) and (f) (SE corner and NE corner of a red box, Washington, D.C. and Baltimore). The x-axis in (f) represents the latitudes along the line AB shown in panel (e). For major spikes, abbreviated names of the power plants are shown (see Figure 3).

Figure 7 because the pixels are so small. Horizontal transects of the CO<sub>2</sub> flux derived from FFDASv2.2 and EDGARv432 exhibit an overall similar shape to those from ACESv1 and ODIAC2018, while spikes induced by power plants are more apparent in the flux transects from ACESv1 and ODIAC2018 due to higher spatial



**Figure 8.** The emission rates of CO<sub>2</sub> from the Balt-Wash area during the sampling period of seven research flights in February 2015. Solid bars and their black vertical lines indicate the seven FLAGG-MD baseline estimates and their 1 $\sigma$  uncertainty range (Table 2). FLAGG-MD mass balance estimates were apportioned to FFCO<sub>2</sub> (purple), non-FFCO<sub>2</sub> anthropogenic emissions (NFA-CO<sub>2</sub>, blue) and the human/pet respiration (yellow) (see Text S5). Dashed bars indicate corresponding FFCO<sub>2</sub> from FFDASv2.2. The black vertical lines at the top of the FFDASv2.2 bars (dashed) indicate the minimum to maximum hourly emission rates of FFCO<sub>2</sub> for each time period, and thus are not an uncertainty estimate of FFDASv2.2.

resolution (Figure 7f). The CT2017 inventory has a 1° lat/lon resolution, and hence the CT2017 map of FFCO<sub>2</sub> is more spatially uniform at the scale of our study domain, since there are only 4 grid cells covering the Balt-Wash area.

According to VEGAS, the net amount of CO<sub>2</sub> emitted by the biogenic sector was ~0.4 MtC in the Balt-Wash area during February 2015. However, the horizontal transect of biogenic CO<sub>2</sub>, simulated by VEGAS and scaled by NDVI (see section 2.4) is nearly constant across the Balt-Wash area during February 2015 (Figure 7f). This horizontal transect for biogenic emissions across our study area indicates that the CO<sub>2</sub> background, defined by the linear fitting method, is likely to already include the enhancement signal due to biogenic emissions. Therefore, we did not attribute any of the CO<sub>2</sub> flux found from the mass balance estimate to the biogenic sector (Figure 8). We acknowledge that the lack of any independent source of validation for VEGAS/NDVI outputs, such as radiocarbon measurements or eddy covariance flux towers, might be a weakness in our analysis. Ongoing efforts to develop <sup>13</sup>CO<sub>2</sub> and radiocarbon measurements from NIST northeast corridor tower network (Karion et al., 2019) and urban biospheric CO<sub>2</sub> models (Hardiman et al., 2017; Smith et al., 2019) will provide further opportunity to study the impact of biogenic CO<sub>2</sub> flux on the aircraft-based mass balance estimates.

### 3.5.2. Hourly Emission Rate of CO<sub>2</sub> From the Baltimore, MD-Washington, D.C. Area

The FLAGG-MD estimate of fossil-fuel combustion CO<sub>2</sub> (FFCO<sub>2</sub>) emission rate is derived from the baseline mass balance estimates shown in Table 2. First, the emissions of CO<sub>2</sub> from human/pet respiration (human, dog, and cat) are estimated based on the following assumptions: the population in the Balt-Wash study area (red box, Figure 7e) was ~8.1 million in February 2015 (CIESIN, 2018); the CO<sub>2</sub> release rate by human respiration is 254 gC/person/day (Prairie & Duarte, 2007); dog/cat ownership is 0.22 dogs/person and 0.24 cats/person, and the dog/cat release rate of CO<sub>2</sub> is 25% of the human release rate (American Veterinary Medical Association, 2012). Next, the estimated emissions from human/pet respiration are subtracted from the baseline mass balance estimates. Then, the remainder of the mass balance estimates was apportioned to either FFCO<sub>2</sub> or Non-FFCO<sub>2</sub> Anthropogenic emissions (hereafter “NFA-CO<sub>2</sub>”) by applying the ratio derived from the Maryland GHG inventory for year 2014 (MDE, 2016). The NFA-CO<sub>2</sub> consists of following sectors: (1) industrial processes (cement manufacture, limestone and dolomite, soda ash, ammonia and urea production), (2) agriculture (urea fertilizer usage), (3) waste management (waste combustion, landfills, and residential open burning). Note that emissions from gasoline for on-road transportation were solely regarded as



FFCO<sub>2</sub>, as the emissions from ethanol (E85) in gasoline comprises only ~0.1% of total emissions from gasoline for on-road transportation (MDE, 2016). See Text S5 for a detailed description of the method utilized for human/pet respiration and the FFCO<sub>2</sub> to Non-FFCO<sub>2</sub> ratio from the Maryland GHG inventory, and their associated uncertainties. Note that we did not apportion any of the mass balance estimates to the biogenic sector, as discussed in section 3.5.1.

Figure 8 shows the emission rates of CO<sub>2</sub> from the Balt-Wash area estimated from seven FLAGG-MD flights and corresponding FFDASv2.2 estimates. On average, FFCO<sub>2</sub> comprises 93% of the mass balance estimates, while NFA-CO<sub>2</sub> and human/pet respiration comprises 4.6% and 2.6%, respectively. Overall, the emission rate of FFCO<sub>2</sub> from FFDASv2.2 for the flight days was 32% larger than that from FLAGG-MD but within the 1 $\sigma$  uncertainty range for most flights, except UMD-RF5. Still, such level of agreement is very meaningful given that FLAGG-MD and FFDASv2.2 use two independent approaches: aircraft observation-based sampling versus a data assimilation framework for disaggregating the annual/national inventory into hourly/0.1° grids.

Turnbull et al. (2018) highlighted that the background CO<sub>2</sub>, determined from the edge fitting method, is likely to be overestimated when there are nonzero emissions over the edge region of the study domain. In their study, CO<sub>2</sub> flux values were computed using an approach similar to equation (1). Then, computed CO<sub>2</sub> flux values were scaled to a background-corrected aircraft mass balance flux by adding a mean CO<sub>2</sub> flux value for the rural area outside the aircraft footprint which was determined from a bottom-up inventory. Should we take the same approach, using either FFDAS or ODIAC to define the emissions of CO<sub>2</sub> along the narrow vertical boxes that define region illustrated in Figure 7, our value of FFCO<sub>2</sub> for the Balt-Wash area would increase by 30%, rising from 1.9 MtC to 2.5 MtC. This type of adjustment is not used in our analysis for two reasons. First, this adjustment implicitly assumes our estimate of background CO<sub>2</sub> is too large by approximately 0.3 ppm, whereas the comparison of the mole fraction of background CO<sub>2</sub> to the measured upwind mole fraction of CO<sub>2</sub> already indicates a potential bias of 0.18 ppm (Figure 2a). If we were to adjust background CO<sub>2</sub> to adjust for possible unaccounted emissions in these edge, rectangular regions, the scatter plot between upwind and background CO<sub>2</sub> would exhibit such a bias that would begin to approach the standard deviation of the difference between upwind and background CO<sub>2</sub>. Second, this adjustment assumes that anthropogenic emissions of CO<sub>2</sub> can be well defined in sparsely populated geographic regions by global models. We are reluctant therefore to make such an adjustment to our estimate of FFCO<sub>2</sub> for the Balt-Wash area, but we acknowledge that our definition of background CO<sub>2</sub> found using the method illustrated in Figure S3 could potentially need revision, due to lack of explicit consideration of anthropogenic emissions of CO<sub>2</sub> in these edge regions. Our approach is similar to the methodology used in numerous other recent mass balance studies (Heimbürger et al., 2017; Krautwurst et al., 2016; Ren et al., 2019).

Finally, we acknowledge that the rectangular-shaped region (Figure 7), determined based on the dominant wind direction, may not perfectly represent the emissions area that induced enhanced CO<sub>2</sub> observed by the aircraft, especially when uncertainties associated with wind variability determination are significant. Such mis-representation of the emissions area could have potentially contributed to the difference between top-down and bottom-up estimates (Lopez-Coto et al., 2020; Turnbull et al., 2018). In this study, flight-by-flight adjustment for the geographic study area was not attempted, as six of the seven flights share similar flight patterns and wind conditions. Unlike the other flights, UMD-RF9 was conducted under north-easterly wind conditions.

### 3.5.3. Monthly Total Emission of CO<sub>2</sub> From the Baltimore, MD-Washington, D.C. Area

The four bottom-up gridded products cover different years (i.e., EDGARv432: 2010, ACESv1: 2014, FFDASv2.2 and ODIAC2018: 2015) with varying temporal resolution (i.e., EDGARv432 and ODIAC2018: monthly, FFDASv2.2 and ACESv1: hourly). To facilitate the comparison among these bottom-up models and our mass balance estimates, the amounts of FFCO<sub>2</sub> emitted during the month of February in the Balt-Wash study area were computed from each bottom-up product and our seven mass balance estimates shown in Figure 8. No further attempts were made to harmonize the temporal mismatch existing in EDGARv432 (year 2010) and ACES v1 (year 2014). The FLAGG-MD monthly total FFCO<sub>2</sub> emission was estimated by temporally scaling up the seven FLAGG-MD emission rates of FFCO<sub>2</sub>, shown in Figure 8. The Temporal Improvements for Modeling Emissions by Scaling (TIMES), which provides scaling factors for diurnal and weekly variability of FFCO<sub>2</sub> in global rectangular 0.25° lat/lon grids, was used for the

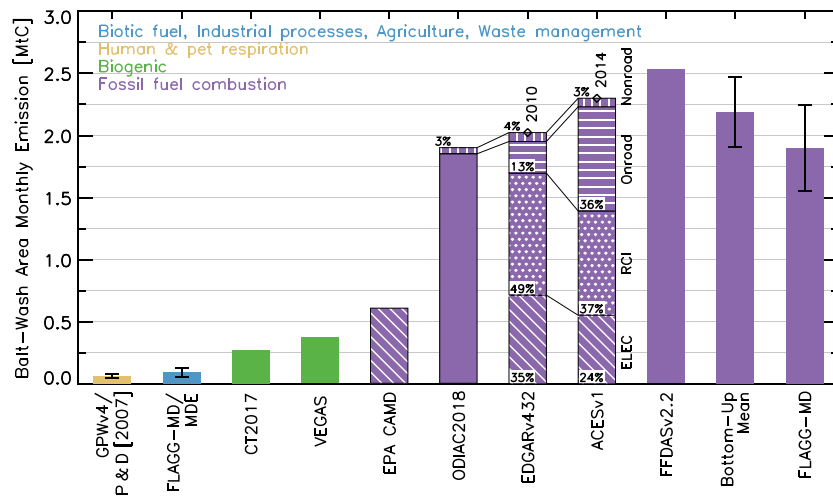


**Figure 9.** Monthly emission of CO<sub>2</sub> from the Balt-wash area for February 2015. The emission by human/pet respiration (yellow) was estimated using population data (GPWv4, (CIESIN, 2018)) and the average respiration rate from Prairie and Duarte (2007) (see Text S5). Non-FFCO<sub>2</sub> anthropogenic emissions (NFA-CO<sub>2</sub>, blue) were calculated from FLAGG-MD mass balance estimates using the scaling factor derived from the MDE GHG inventory 2014 (MDE, 2016). EDGARv432 and ACESv1 were available for 2010 and 2014, respectively. The four bottom-up FFCO<sub>2</sub> estimates (ODIAC2018, EDGARv432, ACESv1, and FFDASv2.2) contain several mismatching emission sectors, and thus are not directly comparable (see text). Sectoral emissions from EDGARv432 and ACESv1 were aggregated into four categories: Electricity generating facilities (“ELEC,” diagonal), residential, commercial, and industrial (“RCI,” dotted), on-road (horizontal) and non-road transportation (vertical). See Text S6 for emission sectors covered by each bottom-up product. The “bottom-up mean” bar and its vertical error bar indicate the mean and standard deviation of the four bottom-up FFCO<sub>2</sub> estimates. The error bar on the FLAGG-MD symbol indicates the 1 $\sigma$  uncertainty range of the best estimate.

temporal scaling process (Nassar et al., 2013). The monthly emissions from human/pet respiration and NFA-CO<sub>2</sub> were estimated as described in section 3.5.2. The major challenge for comparing different bottom-up gridded products is to harmonize various emission source sectors covered by each product (Gately & Hutyra, 2017; Gurney et al., 2019; Oda et al., 2019). In this study, source sector harmonizing was only conducted for EDGARv432 (see Text S6), while all available sectors in other bottom-up products (ACESv1, FFDASv2.2, and ODIAC2018) were used to derive FFCO<sub>2</sub> emissions. Thus, sectoral mismatching among the FLAGG-MD estimate and the four bottom-up products exists for the following sectors: cement manufacturing, gas flaring, aviation, and oil and gas extraction, refining, and transport. These mismatching sectors account for ~4% of the total FFCO<sub>2</sub> in our study domain (see Text S6). Note that one of the main objectives set for developing these global bottom-up gridded products was to provide a prior CO<sub>2</sub> flux for use in inversion modeling (Oda et al., 2018). Therefore, FFCO<sub>2</sub> flux values at specific time-space model grids should be regarded as a climatological mean rather than snapshot of the truth (Gurney, 2018).

We estimate that 2.4 MtC of CO<sub>2</sub> was emitted from the Balt-Wash area during February 2015, according to the FLAGG-MD estimate (all emission other than biogenic) and VEGAS simulations (biogenic CO<sub>2</sub>) (Figure 9). The total 2.4 MtC consists of 1.9 MtC of FFCO<sub>2</sub> (78% of the total), 0.4 MtC of biogenic CO<sub>2</sub> (15%), 0.1 MtC of NFA-CO<sub>2</sub> (4%), and 0.06 MtC of human/pet respiration (3%). The mean and the standard deviation of the four bottom-up estimates of FFCO<sub>2</sub> were  $2.2 \pm 0.3$  MtC (FFDASv2.2: 2.5 MtC, ACESv1: 2.3 MtC, EDGARv432: 2.0 MtC, ODIAC2018: 1.9 MtC), which is 15% larger than the FLAGG-MD estimate of FFCO<sub>2</sub> ( $1.9 \pm 0.3$  MtC). The ODIAC2018 bottom-up estimate of FFCO<sub>2</sub> shows best agreement with the top-down FLAGG-MD estimate.

ACESv1 and EDGARv432 provide sectoral emissions of FFCO<sub>2</sub> for years 2014 and 2010, respectively. Based on ACESv1, power plant emissions were 24% of the monthly total FFCO<sub>2</sub>, while they were 35% of the monthly total FFCO<sub>2</sub> according to EDGARv432 (Figure 9). Estimates from EPA CAMD and FLAGG-MD for our study area suggest power plant emissions accounted for 29% of the monthly total FFCO<sub>2</sub> emissions in February 2015. On-road transportation emissions account for 36% of the ACESv1 estimate, while they

only account for 13% of the EDGARv432 estimate. A significant difference of on-road emissions between ACESv1 and EDGARv432 might be due to the temporal mismatching (i.e., 2010 vs. 2014) of the two inventories but more likely reflects a bias in either one or perhaps both products. Gately et al. (2013) and McDonald et al. (2014) reported that EDGAR overestimates urban vehicles emissions in major U.S. cities. However, the recent update of EDGAR version 4.3.2 addressed this issue by adopting proxy layers for various roads and vehicles types (Janssens-Maenhout et al., 2017). We have not attempted to further quantify the source of the difference between on-road emissions of CO<sub>2</sub> for these two inventories, as this effort is beyond the scope of this study. We leave the detailed analysis of sectoral composition of urban FFCO<sub>2</sub> for future work.

We would like to emphasize that this study provides an independent, objective measure for the emission comparison. Evaluation of downscaled emissions is often difficult mainly due to the lack of physical measurements (Andres et al., 2016; Oda et al., 2018) and often done by inter-comparison of emission inventories that allow only for characterization of differences among inventories. This study demonstrates the use of atmospheric measurements for examining the errors and biases in the emission inventories.

Finally, we compare ODIAC2018, which showed the best agreement against our aircraft-based estimate of the monthly CO<sub>2</sub> emissions, to the Maryland GHG inventory published by the Maryland Department of the Environment (MDE) (2016). The Maryland GHG inventory estimated that 18.8 MtC of FFCO<sub>2</sub> was emitted from Maryland during year 2014, while ODIAC2018 estimated 20.2 MtC for the same domain in 2014. The overall excellent agreement among the top-down approach, bottom-up models, and State emission inventory is promising given the fact that each relies on independent data sets and methodologies.

#### 4. Conclusions

The first FLAGG-MD aircraft campaign was conducted during February 2015 to study the emissions of CO<sub>2</sub> in the Balt-Wash area. Several conclusions are drawn from this study.

First, a series of HYSPLIT transport modeling analyses was conducted to provide source attribution of the plumes of CO<sub>2</sub> observed by the aircraft. A number of plumes of CO<sub>2</sub> could be attributed to either Washington, D.C. and Baltimore, MD, or the major power plants in the study area. We found that inter-state transport of power plant plumes can induce a substantial local increase of CO<sub>2</sub> throughout the Balt-Wash area, increasing the spatial variability of background CO<sub>2</sub>.

Second, the accuracy and precision of the aircraft-based mass balance approach were tested against local power plant emissions, and also the sensitivity of the approach was tested for urban emissions. Emissions of CO<sub>2</sub> from two local power plants were estimated using aircraft data and the resulting estimates were found to have no discernible systematic bias, with a mean percentage error of  $-0.3\%$  compared to corresponding CEMS data for 16 cases. Also, power plants emissions could be estimated with MPE of  $\sim 10\%$  when a total number of 12 plumes was sampled by the aircraft for the mass balance calculation (95% CL). These results demonstrate that the accuracy of mass balance estimates increases and as the number of mass balance experiments increases for the same target emission source (Heimbürger et al., 2017; Karion et al., 2015). From a sensitivity analysis, we found that the variability of the wind speed and direction downwind of the study area have the largest impact on the mass balance calculation, followed by the boundary layer height and the specification of background CO<sub>2</sub>. The  $1\sigma$  uncertainty of a single mass balance estimate of CO<sub>2</sub> emission from the Balt-Wash study area can be significant, ranging from  $\pm 31\%$  to  $\pm 49\%$ . However, we also found that the precision assigned to the mean of the seven mass balance estimates was considerably better, with a SEM95 of  $\pm 16\%$ . This result supports the findings from previous studies: The precision of the mass balance estimate of CO<sub>2</sub> emissions over urban regions is improved by repeating mass balance experiments numerous times, within a short span of time.

Finally, differences among the five bottom-up models (ACESv1, CT2017, EDGARv432, FFDASv2.2, and ODIAC2018) and the top-down estimate were studied from the perspective of both the geographical distribution of CO<sub>2</sub> flux and the total emissions over the Balt-Wash study area. With respect to the geographical distribution of CO<sub>2</sub>, we found that horizontal transects of CO<sub>2</sub> flux across the Balt-Wash area derived from four models (ACESv1, ODIAC2018, EDGARv432, and FFDASv2.2) have similar structures, showing spikes for the area where major power plants and highly developed areas are located. Only ACESv1 provided

spatial distribution of CO<sub>2</sub> flux on the spatial scale of individual roads. From the perspective of total monthly emissions, the FLAGG-MD aircraft flights yield and estimated 1.9 ± 0.3 MtC as the amount of FFCO<sub>2</sub> emitted from the Balt-Wash area during February 2015, and the four bottom-up models (except for CT2017) estimated 2.2 ± 0.3 MtC. ODIAC2018, which provides downscaled emissions for year 2015, shows best agreement with the FLAGG-MD top-down estimate. Evaluation of subnational emissions of bottom-up models is often limited to an evaluation based on an inter-comparison among different models. This study provided an independent, objective measure for the inventory evaluation. Additionally, we found that the statewide annual total FFCO<sub>2</sub> emissions in the Maryland (MDE) GHG inventory was 7% lower than the ODIAC2018 estimate.

Numerous efforts are currently underway to better understand urban emissions of CO<sub>2</sub>. For instance, the recent installations of observation towers and low-cost sensors around the Balt-Wash area will provide improved constraints on spatio-temporal variability of the CO<sub>2</sub> background (Lopez-Coto et al., 2017; Martin et al., 2017, 2019; Mueller et al., 2018). Also, radiocarbon measurements and urban-specific biospheric CO<sub>2</sub> models will provide better understanding on the impact of biogenic CO<sub>2</sub> flux on the aircraft-based mass balance approach. A new version of VEGAS currently under development will incorporate an accurate representation of the diurnal cycle of the biogenic flux of CO<sub>2</sub>. Lastly, frequent and regular aircraft campaigns in the future will provide resources to better understand the gaps among top-down approaches, bottom-up models, and state/local GHG inventories, benefiting both stake holders and the carbon cycle modeling community.

**Acknowledgments**

The FLAGG-MD project was funded and supported by NIST's Greenhouse Gas Measurements program. All aircraft observations data set used in this study are available online (<https://www2.atmos.umd.edu/~flaggmd/>); CarbonTracker CT2017 results provided by NOAA ESRL, Boulder, Colorado, USA from the website online (<http://carbontracker.noaa.gov>). The version of the ODIAC emission data product (ODIAC2018) is available from the Global Environmental Database hosted by the Center for Global Environmental Research (CGER), National Institute for Environmental Studies (NIES), Japan (<http://db.cger.nies.go.jp/dataset/ODIAC/>). Tomohiro Oda is supported by the NASA Carbon Cycle Science Program (grant no. NNX14AM76G). The version of ACES emission data (ACESv1) is available through the Oak Ridge National Laboratory (ORNL) Distributed Active Archive Center (DAAC). The version of the EDGAR emission data (EDGARv4.3.2) is available online (<http://edgar.jrc.ec.europa.eu/overview.php?v=432>) (DOI: [https://data.europa.eu/doi/10.2904/JRC\\_DATASET\\_EDGAR](https://data.europa.eu/doi/10.2904/JRC_DATASET_EDGAR)). Power plants emissions data set (Air Markets Program Data) used in this study is available from U.S. EPA AMPD website (<https://ampd.epa.gov/ampd/>). The authors are grateful to Wenzhe Yang at NOAA for providing NDVI (v1r12) data. We are also grateful for numerous helpful discussions with Anna Karion at NIST. Finally, we sincerely appreciate the helpful comments provided by Jocelyn Turnbull and an anonymous reviewer to the original submitted manuscript.

**Disclaimer**

Certain commercial equipment, instruments, or materials are identified in this paper in order to specify the experimental procedure adequately. Such identification is not intended to imply recommendation or endorsement by the National Institute of Standards and Technology nor is it intended to imply that the materials or equipment identified are necessarily the best available for the purpose.

**References**

American Veterinary Medical Association. (2012). U.S. pet ownership statistics. Retrieved September 7, 2019, from <https://www.avma.org/KB/Resources/Statistics/Pages/Market-research-statistics-US-pet-ownership.aspx>

Andres, R. J., Boden, T. A., & Higdon, D. M. (2016). Gridded uncertainty in fossil fuel carbon dioxide emission maps, a CDIAC example. *Atmospheric Chemistry and Physics*, 16(23). <https://doi.org/10.5194/acp-16-14979-2016>

Asefi-Najafabady, S., Rayner, P. J., Gurney, K. R., McRobert, A., Song, Y., Coltin, K., et al. (2014). A multiyear, global gridded fossil fuel CO<sub>2</sub> emission data product: Evaluation and analysis of results. *Journal of Geophysical Research: Atmospheres*, 119, 10,213–10,231. <https://doi.org/10.1002/2013JD021296>

Bréon, F. M., Broquet, G., Puygrenier, V., Chevallier, F., Xueref-Remy, I., Ramonet, M., et al. (2015). An attempt at estimating Paris area CO<sub>2</sub> emissions from atmospheric concentration measurements. *Atmospheric Chemistry and Physics*, 15(4), 1707–1724. <https://doi.org/10.5194/acp-15-1707-2015>

Cambaliza, M. O. L., Shepson, P. B., Caulton, D. R., Stirm, B., Samarov, D., Gurney, K. R., et al. (2014). Assessment of uncertainties of an aircraft-based mass balance approach for quantifying urban greenhouse gas emissions. *Atmospheric Chemistry and Physics*, 14(17), 9029–9050. <https://doi.org/10.5194/acp-14-9029-2014>

CIESIN (Center for International Earth Science Information Network), C. U. (2018). Gridded population of the world, version 4 (GPWv4): Population count, revision 11. <https://doi.org/10.7927/H4JW8BX5>

Davis, K. J., Deng, A., Lauvaux, T., Miles, N. L., Richardson, S. J., Sarmiento, D. P., et al. (2017). The Indianapolis flux experiment (INFLUX): A test-bed for developing urban greenhouse gas emission measurements. *Elem Sci Anth*, 5(0), 21. <https://doi.org/10.1525/elementa.188>

Department of Energy & Environment. (2018). Clean Energy DC. Retrieved April 10, 2019, from <https://doee.dc.gov/cleanenergydc>

Draxler, R., Hess, G. D., & Air Resources Laboratory (U.S.). (1997). Description of the HYSPLIT\_4 modeling system. Retrieved January 17, 2019, from <https://www.arl.noaa.gov/documents/reports/arl-224.pdf>

Draxler, R., Stunder, B., Rolph, G., Stein, A., & Taylor, A. (2014). *HYSPLIT4 user's Guide Version 4 - Last Revision: September 2014*. University Research Court College Park, Maryland: National Oceanic and Atmospheric Administration (NOAA) Air Resources Laboratory (ARL). Retrieved from [https://www.arl.noaa.gov/data/web/models/hysplit4/win95/user\\_guide.pdf](https://www.arl.noaa.gov/data/web/models/hysplit4/win95/user_guide.pdf)

Duren, R. M., & Miller, C. E. (2012). Measuring the carbon emissions of megacities. *Nature Climate Change*, 2(8), 560–562. <https://doi.org/10.1038/nclimate1629>

Feng, S., Lauvaux, T., Newman, S., Rao, P., Ahmadov, R., Deng, A., et al. (2016). Los Angeles megacity: A high-resolution land-atmosphere modelling system for urban CO<sub>2</sub> emissions. *Atmospheric Chemistry and Physics*, 16(14), 9019–9045. <https://doi.org/10.5194/acp-16-9019-2016>

Gately, C., & Hutrya, L. (2017). Large uncertainties in urban-scale carbon emissions. *Journal of Geophysical Research: Atmospheres*, 122, 11, 242–11, 260. <https://doi.org/10.1002/2017JD027359>

Gately, C., & Hutrya, L. (2018). *CMS: CO<sub>2</sub> Emissions from Fossil Fuels Combustion, ACES Inventory for Northeastern USA*. ORNL DAAC, Oak Ridge, Tennessee, USA: ORNL Distributed Active Archive Center. <https://doi.org/10.3334/orlnl/daac/1501>

- Gately, C. K., Hutyra, L. R., Wing, I. S., & Brondfield, M. N. (2013). A bottom up approach to on-road CO<sub>2</sub> emissions estimates: Improved spatial accuracy and applications for regional planning. *Environmental Science & Technology*, 47(5), 2423–2430. <https://doi.org/10.1021/es304238v>
- Gratani, L., & Varone, L. (2005). Daily and seasonal variation of CO<sub>2</sub> in the city of Rome in relationship with the traffic volume. *Atmospheric Environment*, 39(14), 2619–2624. <https://doi.org/10.1016/j.atmosenv.2005.01.013>
- Gurney, K. (2018). Read me file of Heista fossil fuel carbon dioxide (FFCO<sub>2</sub>) data product - Salt lake country, version 2.2, 0.002 degree grid. Retrieved May 10, 2019, from <https://data.nist.gov/od/ds/696FD547910012A0E0532457068160E41910/readme.002deg.SLC.v2.2.txt>
- Gurney, K., Liang, J., Patarasuk, R., O’Keeffe, D., Huang, J., Hutchins, M., et al. (2017). Reconciling the differences between a bottom-up and inverse-estimated FFCO<sub>2</sub> emissions estimate in a large US urban area. *Elementa: Science of the Anthropocene*, 5, 44. <https://doi.org/10.1525/elementa.137>
- Gurney, K. R., Huang, J., & Coltin, K. (2016). Bias present in US federal agency power plant CO<sub>2</sub> emissions data and implications for the US clean power plan. *Environmental Research Letters*, 11(6), 64,005. <https://doi.org/10.1088/1748-9326/11/6/064005>
- Gurney, K. R., Liang, J., O’Keeffe, D., Patarasuk, R., Hutchins, M., Huang, J., et al. (2019). Comparison of global downscaled versus bottom-up fossil fuel CO<sub>2</sub> emissions at the urban scale in four US urban areas. *Journal of Geophysical Research: Atmospheres*, 124, 2823–2840. <https://doi.org/10.1029/2018JD028859>
- Hardiman, B. S., Wang, J. A., Hutyra, L. R., Gately, C. K., Getson, J. M., & Friedl, M. A. (2017). Accounting for urban biogenic fluxes in regional carbon budgets. *Science of the Total Environment*, 592, 366–372. <https://doi.org/10.1016/j.scitotenv.2017.03.028>
- Heimbürger, A. M. F., Harvey, R. M., Shepson, P. B., Stirm, B. H., Gore, C., Turnbull, J., et al. (2017). Assessing the optimized precision of the aircraft mass balance method for measurement of urban greenhouse gas emission rates through averaging. *Elementa: Science of the Anthropocene*, 5(0), 5. <https://doi.org/10.1525/elementa.134>
- Hutyra, L. R., Duren, R., Gurney, K. R., Grimm, N., Kort, E. A., Larson, E., & Shrestha, G. (2014). Urbanization and the carbon cycle: Current capabilities and research outlook from the natural sciences perspective. *Earths Future*, 2(10), 473–495. <https://doi.org/10.1002/2014ef000255>
- Idso, C. D., Idso, S. B., & Balling Jr, R. C. (2001). An intensive two-week study of an urban CO<sub>2</sub> dome in Phoenix, Arizona, USA. *Atmospheric Environment*, 35(6), 995–1000. [https://doi.org/10.1016/S1352-2310\(00\)00412-X](https://doi.org/10.1016/S1352-2310(00)00412-X)
- Janssens-Maenhout, G., Crippa, M., Guizzardi, D., Muntean, M., Schaaf, E., Dentener, F., et al. (2017). EDGAR v4.3.2 global atlas of the three major greenhouse gas emissions for the period 1970–2012. *Earth System Science Data Discuss*, 2017, 1–55. <https://doi.org/10.5194/essd-2017-79>
- Kalthoff, N., Corsmeier, U., Schmidt, K., Kottmeier, C., Fiedler, F., Habram, M., & Slemr, F. (2002). Emissions of the city of Augsburg determined using the mass balance method. *Atmospheric Environment*, 36, S19–S31. [https://doi.org/10.1016/S1352-2310\(02\)00215-7](https://doi.org/10.1016/S1352-2310(02)00215-7)
- Karion, A., Callahan, W., Stock, M., Prinzivalli, S., Verhulst, K. R., Kim, J., et al. (2019). Greenhouse gas observations from the northeast corridor tower network. *Earth System Science Data Discussions*, 2019, 1–29. <https://doi.org/10.5194/essd-2019-206>
- Karion, A., Sweeney, C., Kort, E. A., Shepson, P. B., Brewer, A., Cambaliza, M., et al. (2015). Aircraft-based estimate of total methane emissions from the Barnett shale region. *Environmental Science & Technology*, 49(13), 8124–8131. <https://doi.org/10.1021/acs.est.5b00217>
- Krautwurst, S., Gerilowski, K., Jonsson, H. H., Thompson, D. R., Kolyer, R. W., Thorpe, A. K., et al. (2016). Methane emissions from a Californian landfill, determined from airborne remote sensing and in-situ measurements. *Atmospheric Measurement Techniques Discussions*, 2016, 1–33. <https://doi.org/10.5194/amt-2016-391>
- Lauvaux, T., Miles, N. L., Deng, A., Richardson, S. J., Cambaliza, M. O., Davis, K. J., et al. (2016). High-resolution atmospheric inversion of urban CO<sub>2</sub> emissions during the dormant season of the Indianapolis flux experiment (INFLUX). *Journal of Geophysical Research: Atmospheres*, 121, 5213–5236. <https://doi.org/10.1002/2015JD024473>
- Lopez-Coto, I., Ghosh, S., Prasad, K., & Whetstone, J. (2017). Tower-based greenhouse gas measurement network design—The National Institute of Standards and Technology north east corridor Testbed. *Advances in Atmospheric Sciences*, 34(9), 1095–1105. <https://doi.org/10.1007/s00376-017-6094-6>
- Lopez-Coto, I., Ren, X., Salmon, O. E., Karion, A., Shepson, P. B., Dickerson, R. R., et al. (2020). Wintertime CO<sub>2</sub>, CH<sub>4</sub> and CO emissions estimation for the Washington DC/Baltimore metropolitan area using an inverse modeling technique. *Environmental Science & Technology*, 54(5), 2606–2614. <https://doi.org/10.1021/acs.est.9b06619>
- Martin, C. R., Zeng, N., Karion, A., Dickerson, R. R., Ren, X., Turpie, B. N., & Weber, K. J. (2017). Evaluation and enhancement of a low-cost NDIR CO<sub>2</sub> sensor. *Atmospheric Measurement Techniques Discussions*, 2017, 1–25. <https://doi.org/10.5194/amt-2016-396>
- Martin, C. R., Zeng, N., Karion, A., Mueller, K., Ghosh, S., Lopez-Coto, I., et al. (2019). Investigating sources of variability and error in simulations of carbon dioxide in an urban region. *Atmospheric Environment*, 199, 55–69. <https://doi.org/10.1016/j.atmosenv.2018.11.013>
- McDonald, B. C., McBride, Z. C., Martin, E. W., & Harley, R. A. (2014). High-resolution mapping of motor vehicle carbon dioxide emissions. *Journal of Geophysical Research: Atmospheres*, 119, 5283–5298. <https://doi.org/10.1002/2013JD021219>
- McKain, K., Wofsy, S. C., Nehrkorn, T., Eluszkiewicz, J., Ehleringer, J. R., & Stephens, B. B. (2012). Assessment of ground-based atmospheric observations for verification of greenhouse gas emissions from an urban region. *Proceedings of the National Academy of Sciences of the United States of America*, 109(22), 8423–8428. <https://doi.org/10.1073/pnas.1116645109>
- Maryland Department of the Environment. (2015). The Greenhouse Gas Emissions Reduction Act Plan Update 2015. Retrieved March 17, 2019, from <https://mde.maryland.gov/programs/marylander/documents/mccc/publications/2015ggrplanupdate/climateupdate2015.pdf>
- MDE (Maryland Department of the Environment). (2016). Maryland 2014 Periodic GHG Emissions Inventory. Retrieved August 1, 2018, from <https://mde.state.md.us/programs/Air/ClimateChange/Pages/GreenhouseGasInventory.aspx>
- Mueller, K., Yadav, V., Lopez-Coto, I., Karion, A., Gourdji, S., Martin, C., & Whetstone, J. (2018). Siting background towers to characterize incoming air for urban greenhouse gas estimation: A case study in the Washington, DC/Baltimore area. *Journal of Geophysical Research: Atmospheres*, 123, 2910–2926. <https://doi.org/10.1002/2017JD027364>
- Nassar, R., Napier-Linton, L., Gurney, K. R., Andres, R. J., Oda, T., Vogel, F. R., & Deng, F. (2013). Improving the temporal and spatial distribution of CO<sub>2</sub> emissions from global fossil fuel emission data sets. *Journal of Geophysical Research: Atmospheres*, 118, 917–933. <https://doi.org/10.1029/2012JD018196>
- Newman, S., Xu, X., Gurney, K. R., Hsu, Y. K., Li, K. F., Jiang, X., et al. (2016). Toward consistency between trends in bottom-up CO<sub>2</sub> emissions and top-down atmospheric measurements in the Los Angeles megacity. *Atmospheric Chemistry and Physics*, 16(6), 3843–3863. <https://doi.org/10.5194/acp-16-3843-2016>

- O'Shea, S. J., Allen, G., Fleming, Z. L., Bauguitte, S. J. B., Percival, C. J., Gallagher, M. W., et al. (2014). Area fluxes of carbon dioxide, methane, and carbon monoxide derived from airborne measurements around Greater London: A case study during summer 2012. *Journal of Geophysical Research: Atmospheres*, *119*, 4940–4952. <https://doi.org/10.1002/2013JD021269>
- Oda, T., & Maksyutov, S. (2011). A very high-resolution (1 km×1 km) global fossil fuel CO<sub>2</sub> emission inventory derived using a point source database and satellite observations of nighttime lights. *Atmospheric Chemistry and Physics*, *11*(2), 543–556. <https://doi.org/10.5194/acp-11-543-2011>
- Oda, T., & Maksyutov, S. (2015). ODIAC fossil fuel CO<sub>2</sub> emissions dataset, Center for Global Environmental Research, National Institute for Environmental Studies. <https://doi.org/10.17595/20170411.001> (access date: 2019/03/27).
- Oda, T., Maksyutov, S., & Andres, R. J. (2018). The open-source data inventory for anthropogenic CO<sub>2</sub>, version 2016 (ODIAC2016): A global monthly fossil fuel CO<sub>2</sub> gridded emissions data product for tracer transport simulations and surface flux inversions. *Earth System Science Data*, *10*(1), 87–107. <https://doi.org/10.5194/essd-10-87-2018>
- Oda, T., Bun, R., Kinakh, V., Topylko, P., Halushchak, M., Marland, G., et al. (2019). Errors and uncertainties in a gridded carbon dioxide emissions inventory. *Mitigation and Adaptation Strategies for Global Change*, *24*(6), 1007–1050. <https://doi.org/10.1007/s11027-019-09877-2>
- Patarasuk, R., Gurney, K. R., O'Keeffe, D., Song, Y., Huang, J., Rao, P., et al. (2016). Urban high-resolution fossil fuel CO<sub>2</sub> emissions quantification and exploration of emission drivers for potential policy applications. *Urban Ecosystem*, *19*(3), 1013–1039. <https://doi.org/10.1007/s11252-016-0553-1>
- Peischl, J., Karion, A., Sweeney, C., Kort, E. A., Smith, M. L., Brandt, A. R., et al. (2016). Quantifying atmospheric methane emissions from oil and natural gas production in the Bakken shale region of North Dakota. *Journal of Geophysical Research: Atmospheres*, *121*, 6101–6111. <https://doi.org/10.1002/2015JD024631>
- Peters, W., Jacobson, A. R., Sweeney, C., Andrews, A. E., Conway, T. J., Masarie, K., et al. (2007). An atmospheric perspective on north American carbon dioxide exchange: CarbonTracker. *Proceedings of the National Academy of Sciences*, *104*(48), 18,925–18,930. <https://doi.org/10.1073/pnas.0708986104>
- Prairie, Y. T., & Duarte, C. M. (2007). Direct and indirect metabolic CO<sub>2</sub> release by humanity. *Biogeosciences*, *4*(2), 215–217. <https://doi.org/10.5194/bg-4-215-2007>
- Quick, J. C., & Marland, E. (2019). Systematic error and uncertain carbon dioxide emissions from US power plants. *Journal of the Air & Waste Management Association*, 1–13. <https://doi.org/10.1080/10962247.2019.1578702>
- Rayner, P. J., Raupach, M. R., Paget, M., Peylin, P., & Koffi, E. (2010). A new global gridded data set of CO<sub>2</sub> emissions from fossil fuel combustion: Methodology and evaluation. *Journal of Geophysical Research*, *115*, D19306. <https://doi.org/10.1029/2009JD013439>
- Ren, X., Hall D. L., Vinciguerra T., Benish S. E., Stratton P. R., Ahn D., et al. (2019). Methane emissions from the Marcellus shale in southwestern Pennsylvania and northern west Virginia based on airborne measurements. *Journal of Geophysical Research: Atmospheres*, *124*, 3, 1862, 1878 <https://doi.org/10.1029/2018JD029690>
- Ren, X., Salmon, O. E., Hansford, J. R., Ahn, D., Hall, D., Benish, S. E., et al. (2018). Methane emissions from the Baltimore-Washington area based on airborne observations: Comparison to emissions inventories. *Journal of Geophysical Research: Atmospheres*, *123*, 8869–8882. <https://doi.org/10.1029/2018JD028851>
- Salawitch, R. J., Canty, T. P., Hope, A. P., Tribett, W. R., & Bennett, B. F. (2017). *Paris climate agreement: Beacon of hope*. Cham, Switzerland: Springer International Publishing. <https://doi.org/10.1007/978-3-319-46939-3>
- Salmon, O. E., Shepson, P. B., Ren, X., He, H., Hall, D. L., Dickerson, R. R., et al. (2018). Top-down estimates of NO<sub>x</sub> and CO emissions from Washington, DC-Baltimore during the WINTER campaign. *Journal of Geophysical Research: Atmospheres*, *123*, 7705–7724. <https://doi.org/10.1029/2018JD028539>
- Salmon, O. E., Shepson, P. B., Ren, X., Marquardt Collow, A. B., Miller, M. A., Carlton, A. G., et al. (2017). Urban emissions of water vapor in winter. *Journal of Geophysical Research: Atmospheres*, *122*, 9467–9484. <https://doi.org/10.1002/2016JD026074>
- Sargent, M., Barrera, Y., Nehrkorn, T., Hutyra, L. R., Gately, C. K., Jones, T., et al. (2018). Anthropogenic and biogenic CO<sub>2</sub> fluxes in the Boston urban region. *Proceedings of the National Academy of Sciences*, *115*(29), 7491–7496. <https://doi.org/10.1073/pnas.1803715115>
- Smith, I. A., Hutyra, L. R., Reinmann, A. B., Thompson, J. R., & Allen, D. W. (2019). Evidence for edge enhancements of soil respiration in temperate forests. *Geophysical Research Letters*, *46*(8), 4278–4287. <https://doi.org/10.1029/2019GL082459>
- Stein, A. F., Draxler, R. R., Rolph, G. D., Stunder, B. J. B., Cohen, M. D., & Ngan, F. (2015). NOAA's HYSPLIT atmospheric transport and dispersion modeling system. *Bulletin of the American Meteorological Society*, *96*(12), 2059–2077. <https://doi.org/10.1175/BAMS-D-14-00110.1>
- Stocker, T. F., Qin, D., Plattner, G.-K., Tignor, M., Allen, S. K., Boschung, J., et al. (2013). IPCC, 2013: Climate Change 2013: The Physical Science Basis. Contribution of Working Group I to the Fifth Assessment Report of the Intergovernmental Panel on Climate Change. Retrieved November 28, 2018, from <https://www.ipcc.ch/report/ar5/wg1/>
- Strong, C., Stwertka, C., Bowling, D. R., Stephens, B. B., & Ehleringer, J. R. (2011). Urban carbon dioxide cycles within the Salt Lake Valley: A multiple-box model validated by observations. *Journal of Geophysical Research*, *116*, D15307. <https://doi.org/10.1029/2011JD015693>
- Trainer, M., Ridley, B. A., Buhr, M. P., Kok, G., Walega, J., Hübler, G., et al. (1995). Regional ozone and urban plumes in the southeastern United-States - Birmingham, a case-study. *Journal of Geophysical Research*, *100*(D9), 18823–18,834. <https://doi.org/10.1029/95JD01641>
- Turnbull, J., Karion, A., Davis, K. J., Lauvaux, T., Miles, N. L., Richardson, S. J., et al. (2018). Synthesis of urban CO<sub>2</sub> emission estimates from multiple methods from the Indianapolis Flux Project (INFLUX). *Environmental Science & Technology*, *53*(1), 287–295. <https://doi.org/10.1021/acs.est.8b05552>
- Turnbull, J., Sweeney, C., Karion, A., Newberger, T., Lehman, S. J., Tans, P. P., et al. (2015). Toward quantification and source sector identification of fossil fuel CO<sub>2</sub> emissions from an urban area: Results from the INFLUX experiment. *Journal of Geophysical Research: Atmospheres*, *120*, 292–312. <https://doi.org/10.1002/2014JD022555>
- UN (United Nations). (2017). Reference: C.N.464.2017.TREATIES-XXVII.7.d (Depositary Notification). Retrieved May 10, 2019, from <https://treaties.un.org/doc/Publication/CN/2017/CN.464.2017-Eng.pdf>
- UN-Habitat (United Nations Human Settlements Programme). (2011). *Cities and climate change: Global report on human settlements 2011* (Illustrate). Earthscan. Retrieved from <https://books.google.com/books?id=dzJhJny37h8C>
- USEIA (US Energy Information Administration). (2016). Layer Information for Interactive State Maps: Power Plants. Retrieved March 1, 2016, from [https://www.eia.gov/maps/layer\\_info-m.php](https://www.eia.gov/maps/layer_info-m.php)
- USEPA (U.S. Environmental Protection Agency). (2009). Plain English Guide to the Part 75 Rule. Retrieved May 10, 2019, from [https://www.epa.gov/sites/production/files/2015-05/documents/plain\\_english\\_guide\\_to\\_the\\_part\\_75\\_rule.pdf](https://www.epa.gov/sites/production/files/2015-05/documents/plain_english_guide_to_the_part_75_rule.pdf)
- USEPA AMPD (U.S. Environmental Protection Agency). (2015). Air Markets Program Data (AMPD). Retrieved August 1, 2015, from <https://ampd.epa.gov/ampd/>

- USEPA GHGRP (U.S. Environmental Protection Agency). (2019). Greenhouse Gas Reporting Program (GHGRP). Retrieved March 1, 2017, from <https://www.epa.gov/ghgreporting>
- Whetstone, J. R. (2018). Advances in urban greenhouse gas flux quantification: The Indianapolis flux experiment (INFLUX). *Elementa: Science of the Anthropocene*, 6(1). <https://doi.org/10.1525/elementa.282>
- White, W. H., Patterson, D. E., & Wilson, W. E. (1983). *Urban Exports to the Nonurban Troposphere: Results from Project MISTT*. *Journal of Geophysical Research: Oceans*, 88, C15, 10745. <https://doi.org/10.1029/JC088iC15p10745>
- Zeng, N., Mariotti, A., & Wetzel, P. (2005). Terrestrial mechanisms of interannual CO<sub>2</sub> variability. *Global Biogeochemical Cycles*, 19(1). <https://doi.org/10.1029/2004GB002273>
- Zeng, N., Qian, H., Munoz, E., & Iacono, R. (2004). How strong is carbon cycle-climate feedback under global warming? *Geophysical Research Letters*, 31(20). <https://doi.org/10.1029/2004GL020904>